Theses and Dissertations   1. Thesis and Dissertation Collection, all items

1995-12

Analytical analysis of tip travel in a Bourdon tube

Conway, Cynthia D.

Monterey, California. Naval Postgraduate School

http://hdl.handle.net/10945/31294

NAVAL POSTGRADUATE SCHOOL
MONTEREY, CALIFORNIA

THESIS

**ANALYTICAL ANALYSIS OF TIP TRAVEL
IN A BOURDON TUBE**

by

Cynthia D. Conway

December, 1995

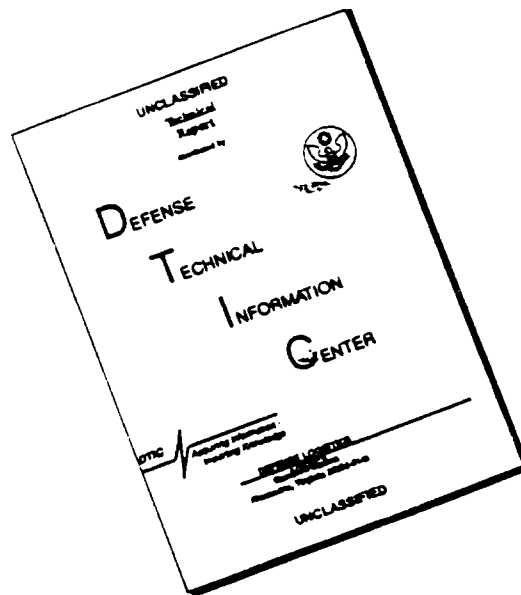Thesis Advisor: R. Mukherjee

Approved for public release; distribution is unlimited.

19960401 067

DISCLAIMER NOTICE

THIS DOCUMENT IS BEST QUALITY AVAILABLE. THE COPY FURNISHED TO DTIC CONTAINED A SIGNIFICANT NUMBER OF PAGES WHICH DO NOT REPRODUCE LEGIBLY.

REPORT DOCUMENTATION PAGE

Form Approved OMB No. 0704-0188

1. AGENCY USE ONLY *(Leave blank)*	2. REPORT DATE December, 1995	3. REPORT TYPE AND DATES COVERED Master's Thesis

4. TITLE AND SUBTITLE ANALYTICAL ANALYSIS OF TIP TRAVEL IN A BOURDON TUBE	5. FUNDING NUMBERS
6. AUTHOR(S) Cynthia D. Conway	

7. PERFORMING ORGANIZATION NAME(S) AND ADDRESS(ES) Naval Postgraduate School Monterey CA 93943-5000	8. PERFORMING ORGANIZATION REPORT NUMBER

9. SPONSORING/MONITORING AGENCY NAME(S) AND ADDRESS(ES)	10. SPONSORING/MONITORING AGENCY REPORT NUMBER

11. SUPPLEMENTARY NOTES The views expressed in this thesis are those of the author and do not reflect the official policy or position of the Department of Defense or the U.S. Government.

12a. DISTRIBUTION/AVAILABILITY STATEMENT Approved for public release; distribution is unlimited.	12b. DISTRIBUTION CODE

13. ABSTRACT *(maximum 200 words)*
Bourdon tubes are the most commonly used elastic elements in mechanical pressure gauges. Basic theory describing the principles of Bourdon behavior is readily available but very few analytical studies have been published that model Bourdon element behavior. The purpose of this research is to develop an analytical model to determine tip displacement in tubular elastic elements using basic principles of solid mechanics. To determine the validity of the results obtained from the analytical model, a study of results from finite element solutions and experimental data is also presented.

14. SUBJECT TERMS Bourdon tubes, finite element solutions, energy methods	15. NUMBER OF PAGES 102
	16. PRICE CODE

17. SECURITY CLASSIFICATION OF REPORT Unclassified	18. SECURITY CLASSIFICATION OF THIS PAGE Unclassified	19. SECURITY CLASSIFICATION OF ABSTRACT Unclassified	20. LIMITATION OF ABSTRACT UL

NSN 7540-01-280-5500

Standard Form 298 (Rev. 2-89)
Prescribed by ANSI Std. 239-18 298-102

Approved for public release; distribution is unlimited.

ANALYTICAL ANALYSIS OF TIP TRAVEL
IN A BOURDON TUBE

Cynthia D. Conway
Lieutenant, United States Navy
B.S., Clemson University, 1990

Submitted in partial fulfillment
of the requirements for the degree of

MASTER OF SCIENCE IN MECHANICAL ENGINEERING

from the

NAVAL POSTGRADUATE SCHOOL
December 1995

Author: _____
Cynthia D. Conway

Approved by: _____
Ranjan Mukherjee, Thesis Advisor

_____
Matthew D. Kelleher, Chairman
Department of Mechanical Engineering

iii

ABSTRACT

Bourdon tubes are the most commonly used elastic elements in mechanical pressure gauges. Basic theory describing the principles of Bourdon behavior is readily available but very few analytical studies have been published that model Bourdon element behavior. The purpose of this research is to develop an analytical model to determine tip displacement in tubular elastic elements using basic principles of solid mechanics. To determine the validity of the results obtained from the analytical model, a study of results from finite element solutions and experimental data is also presented.

TABLE OF CONTENTS

LIST OF TABLES

x

LIST OF FIGURES

I. INTRODUCTION

A. MOTIVATIONS FOR THIS RESEARCH

Bourdon tubes, the elastic elements used in mechanical pressure gauges, are quite popular, even today, due to their simplicity. When a Bourdon tube is fabricated from conventional alloys and operated within its elastic limit, the tip of the tube moves a small distance. However, if the Bourdon element were fabricated from a superelastic alloy capable of withstanding strains on the order of 8%, strains much higher than what ordinary alloys can withstand, the Bourdon tube could be used in unconventional applications as a robotic finger or as an actuator. With these unique applications in mind, the study of the elastic deformation of a Bourdon tube was initiated.

The efforts of a literature survey, the results of which are discussed later in this chapter, yielded little information in terms of analytical solutions to Bourdon tube behavior. In industries that manufacture Bourdon tubes, tip travel is obtained from experimental data in the absence of a mathematical model. This further prompted the development of an analytical solution for tip travel in a Bourdon tube.

With today's micro-chip technology, many people think that the trend for pressure gauges is moving in the direction of the electronic transducer. Surprisingly, precision pressure gauges demonstrate consistent and accurate behavior using Bourdon tube technology. As a result, the demand for Bourdon gauges is quite significant. The most obvious advantages characteristic of Bourdon gauges are their (1) broad pressure range, (2) low cost compared to electronic gauges, (3) ease of manufacturing, (4) ease of

1

operation, (5) ease of troubleshooting, (6) good accuracy (up to 0.1 % full scale deflection), and (7) lack of an external power source which precludes susceptibility to line noise and power outages. [Ref. 1,2]

Bourdon tubes are extremely popular as elastic elements in pressure gauges. Despite their popularity little analytical work has been performed or published modeling their behavior. The work presented in this thesis provides such an analysis.

B. BOURDON TUBE BEHAVIOR

1. Developmental History

In 1849, a French engineer named Eugene Bourdon invented the C-shaped element commonly known today as the Bourdon tube or C spring. While witnessing the construction of a steam engine, Eugene Bourdon noticed that the helically wound coil used to condense the steam was flattened during formation. To correct the deformation, the tube was plugged at one end and pressurized at the other. As a result, the coil partially unwound as the flattened tube regained its circular cross-section. Intrigued by what he saw, Eugene Bourdon conducted his own experiments and eventually invented a pressure gauge using the tip deflection of a curved tube with an elliptical cross section as a pressure measuring device. [Ref. 1] Figure 1 offers an exploded view of a typical C-type pressure gauge.

2. Deflection Theory

The Bourdon tube, henceforth referred to as the Bourdon, is the actuating element in many pressure measuring devices. Typically, the Bourdon elastic element has an oval

Bourdon tube

Tip

Case

Stem (socket)

Pressure
connection

Pressure Element
Assembly Detail

Link

Movement

Pressure Element
Assembly

Scale
(graduations)

Dial

Stop pin

Pointer

Window

Ring

Assembled Pressure Gauge
(Typical)
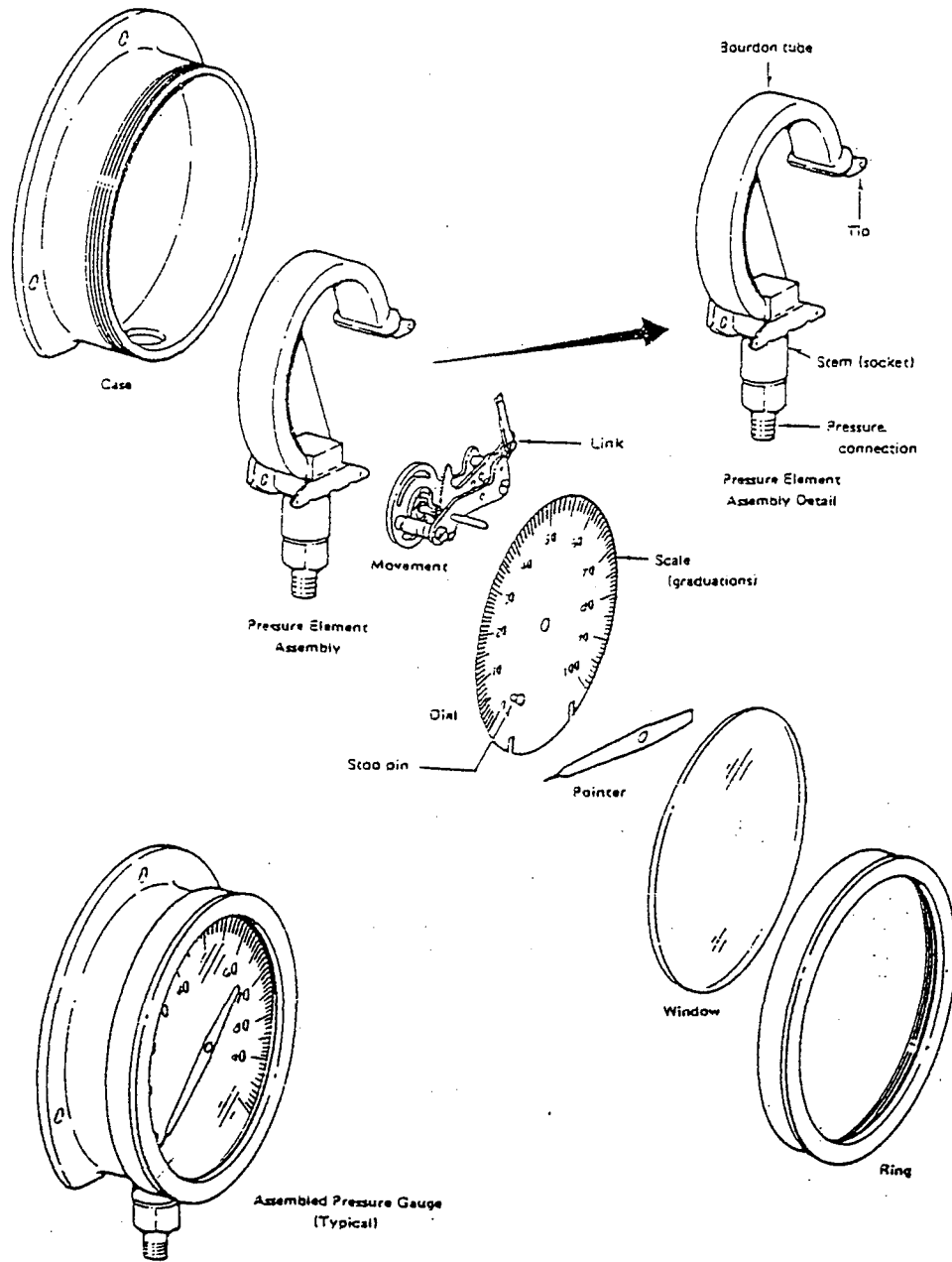
Figure 1. C-type Bourdon gauge

3

or elliptical cross-section and is coiled in the shape of a C, a spiral, or a helix as shown in Figure 2. One end of the tube is sealed and the other is connected to a capillary tube through which pressure is applied. Any pressure within the tube in excess of the external or atmospheric pressure causes the flattened element to elastically change its shape to a more circular cross-section. The resulting change in the cross-section causes the coiled tube to straighten. With one end of the tube fixed, the straightening effect causes the free end to move a small distance. This small, unenhanced movement is called tip travel as shown in Figure 3. [Ref. 1,3,4,5,6]

In a C-type Bourdon, the elastic deformation of the cross-section creates compressive stresses along the inner wall and tensile stresses along the outer wall as defined in Figure 3. When added to the tensile stresses existing in both walls due to the applied internal pressure, a stress imbalance is created such that the tensile stress in the outer wall is greater than the tensile stress in the inner wall. In the process of straightening, the tube experiences tensile stresses in the inner wall and compressive stresses in the outer wall, just the opposite caused by the change in cross-section. The effect of straightening relieves the unbalanced stress condition created by the change in cross-section. The free end of the Bourdon moves with the application of pressure until opposing stresses within the tube reach equilibrium. [Ref. 1,4,5]

3. Design Criteria

As stated earlier, the first Bourdon pressure gauge was patented more than 100 years ago. But despite its age and the fact that "technology" is now much more

4
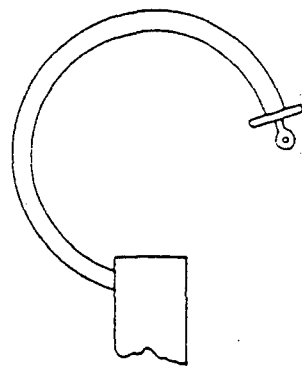
C-Type Bourdon Tube.
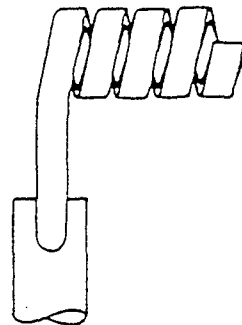
Helical Bourdon Tube

Spiral Bourdon Tube

Figure 2. Common Bourdon elastic elements

5

DIRECTION
OF
MOTION

OUTER WALL
(TENSILE STRESS)

TIP
TRAVEL

INNER WALL
(COMPRESSIVE STRESS)

(a)

MAJOR AXIS

MINOR AXIS

SECTION A-A

(b)
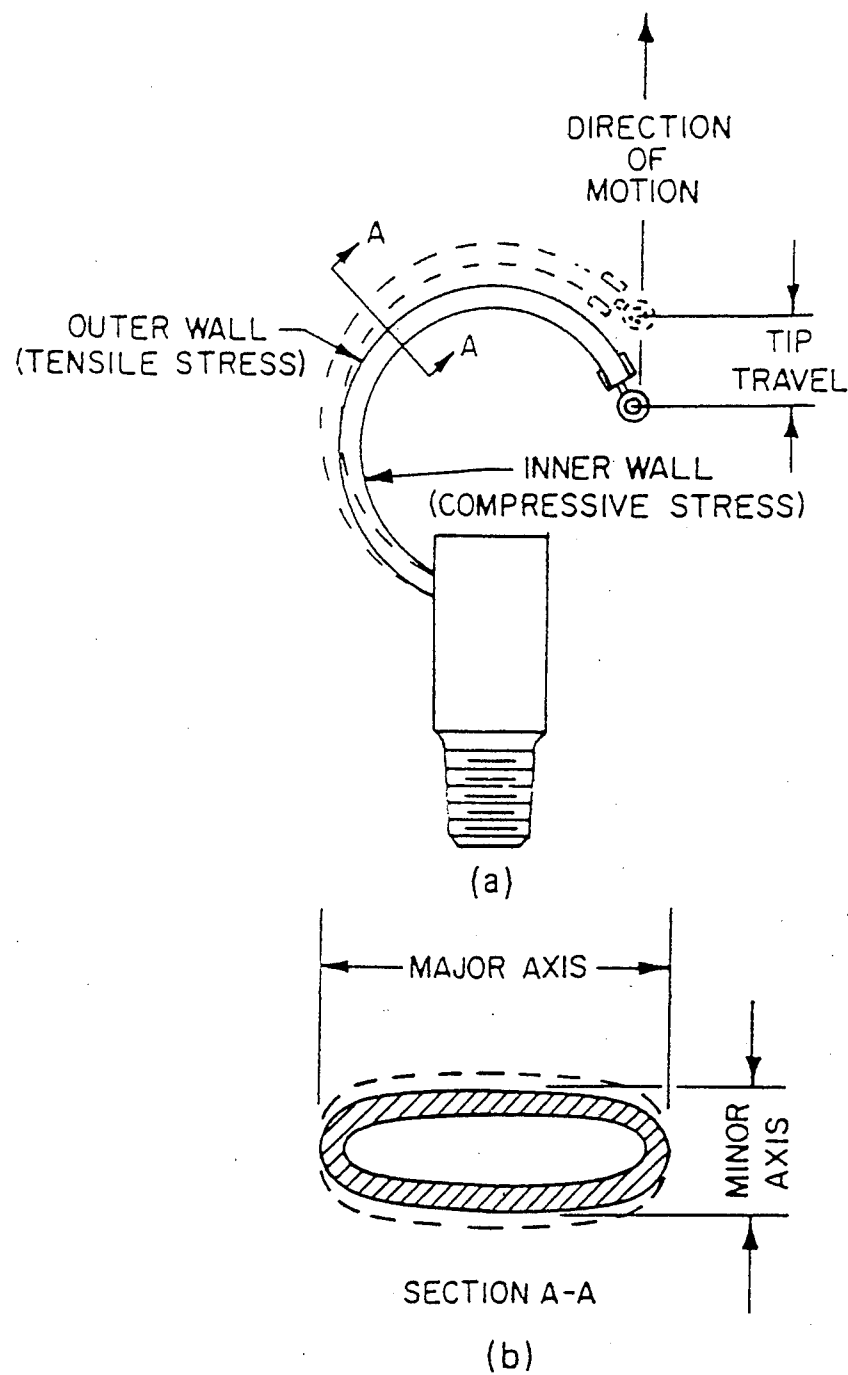
Figure 3. Description of tip travel in a Bourdon element (from Ref. 1)

6

advanced, very little about the design of a Bourdon gauge has changed. The factors considered most important in the design of tubular elastic elements are (1) the element material, (2) the coil length, (3) the wall thickness of the tube, (4) the cross-sectional shape, and (5) the desired tip travel.

Bourdons may be made of ferrous or nonferrous metals depending on the application of the gauge. Admiralty brass, phosphor bronze, and beryllium copper, which are used to make grade B accuracy gauges, higher quality grade A and AA gauges, and high pressure gauges, respectively, are examples of nonferrous metals applications. Ni-Span C is a popular but expensive ferrous material used for its exceptional temperature behavior. [Ref. 1]

As stated earlier, Bourdon elements may be coiled in the shape of a C, a spiral, or a helix. The shape and coil length of the elastic element depends on the pressure range of operation. For pressures up to 60 bar (6 MPa, 870.24 psi), C-type elements are typically used and for pressures above 60 bar, spiral or helical elements are used.
[Ref. 5]

The geometry of the cross-section, one factor affecting tip displacement, is chosen depending on the pressure range of operation. The distinction is made between low and high pressure measuring elements for the proper choice of the wall thickness. Low pressure gauges are loosely defined as those operating from 12 - 500 psi and typically have flatter cross-sections and thinner walls than high pressure gauges which have rounder cross-sections and thicker walls and may read pressures as high as 100,000

7

psi. [Ref. 6] Low pressure Bourdons experience greater tip travel for a given pressure whereas high pressure Bourdons exert higher tip forces. [Ref. 1]

Tip travel in a Bourdon element varies widely with the range of the gauge. Low pressure gauges, with thinner walls and smaller minor axes, are less effective in overcoming the frictional forces within the amplifying movement. Higher tip travel and smaller amplification means smoother pointer motion but also produces excessive stresses in high pressure elements. As a result, high pressure gauges have thicker walls, larger minor axes, and high amplification movements to keep tip travel small. Gauge manufacturers design their Bourdon elements for specific magnitudes of tip deflection. For ease of manufacturing and maintenance, variations in design are kept to a minimum. As a result, the major distinction between gauges is found within the movement mechanisms.

When designing their gauges, manufacturers either determine the appropriate length of the sector tail and the gear ratio necessary to produce the pointer rotation for the desired tip travel or determine the necessary tip travel to operate a specific movement. [Ref. 1, 2, 3, 4, 5] Bourdon tip displacement is generally linear with pressure such that 25%, 50%, and 75% of the total applied pressure is equal to 25%, 50%, and 75% of the total tip displacement. Non-linearities in tip displacement are compensated by varying bourdon geometry or by adjusting the movement.

4. Temperature Effects

One of the most difficult problems that manufacturers of precision pressure gauges must overcome is the effects of temperature on the elastic element. Tip

displacement is very susceptible to changes in ambient temperature. The temperature characteristics of a Bourdon depend on geometry and material. Fluctuations in temperature affect the elastic modulus, or stiffness, of the bourdon. Higher temperatures correspond to lower stiffnesses which mean greater tip travel. The opposite is also true.

Thermal length changes affect the entire measuring system. The easiest and cheapest way to compensate for temperature effects is to manufacture elastic elements from materials having low coefficients of thermal expansion. The material most commonly used for this purpose is Ni-Span C. Although less affected by temperature, Ni-Span C does not completely eliminate the effects of temperature. Manufacturers also compensate for temperature effects by making all of the components of the measuring device from the same material. This approach eliminates any tip deflection relative to the movement caused by temperature changes. [Ref. 2,4]

Some gauge manufacturers maintain gauge accuracy across fluctuating temperatures with the addition of a temperature compensator within the movement mechanism. The device reacts to the same temperature that affects the bourdon. As the temperature changes, the device adjusts a setting within the movement to offset the temperature effect. Each compensator is custom manufactured to match and offset the temperature characteristics of the elastic element with which it is used. [Ref. 2]

5. Technical Publications

Only one publication was found that presented an analytical solution for bourdon behavior. In 1946, Alfred Wolf wrote *An Elementary Theory of the Bourdon Gage* which presented theory based on two elements of strain: strain due to "the bending of the walls

in a transverse section through the tubing" and to "longitudinal extension and contraction parallel to the axis of the tubing". In this publication, Wolf derived formulas for what he called the sensitivity ($\delta R/R$) and the torque (T) of the bourdon where δR was defined as the change in radius of curvature and torque was defined as the external bending moment required to restore tip deflection to zero for any given pressure. Based upon his theoretical results, Wolf concluded that the theory of pure bending in thin shells did not adequately model the behavior of the bourdon for the case a^4/R^2t^2 much greater than unity and that gauge sensitivity was inversely proportional to the first power of t for thin-walled tubes. Wolf's tabulated results for "observed" and "calculated" sensitivities and torques for a steel elastic element were quite comparable to on another.

6. Manufacturers' Literature

The logical progression in the search for literature was contacting companies that manufacture the elastic elements addressed and analyzed in this paper. A representative from the Stewart Warner Instrument Corporation commented that their gauges cover a very broad range of pressures and are "old standards" based on tried and true designs. On the rare occasion that a customer requests a pressure gauge not previously manufactured, the company has a "formula" for estimating the new design based on established gauge designs. The company representative also said he had no knowledge of an analytical model to determine tip travel.

Excerpts from a pressure measurement handbook produced by the WIKA Instrument Corporation provided a brief history, the principles of operation, some design considerations, the effects of temperature, and load constraints of bourdon gauges. The

10

excerpts also presented equations for tip travel, relative change in curvature, and maximum bending stresses of tubular elements but, for proprietary reasons, all were expressed as functions of undefined variables.

The Heise Division of Dresser Industries also provided some literature on dial gauges. Their biggest contribution to this literature survey was information concerning temperature compensation, methods of which were previously discussed. Like the Stewart Warner Corporation, Heise's gauges are well established and rooted in 50-year old designs. Heise is, however, currently developing its own analytical model for Bourdon elements.

The efforts of a literature survey yielded relatively little information concerning analytical studies of Bourdon pressure gauges. Very few technical papers have been published which analytically describe Bourdon theory. As a result, gauge manufacturers typically rely on experimentation and established designs when creating new gauges.

C. RESEARCH OBJECTIVES

The objectives of this research were to develop an analytical solution for tip travel, specifically in C-type Bourdons, and to compare results from the analytical model to results from finite element models and data collected from laboratory experiments. Because pressure gauge manufacturers most commonly rely on experimentation for the design of new gauges, a realization of the stated objectives could prove to be quite useful to them or to anyone interested in the applications of Bourdon theory.

II. ANALYTICAL ANALYSIS OF A BOURDON TUBE

A. NOMENCLATURE AND ASSUMPTIONS

1. Nomenclature

For clarity, symbols related to Bourdon geometry are annotated in Figure 4 and defined as follows:

a - semi-major axis of the elliptical cross-section

b - semi-minor axis of the elliptical cross-section

t - wall thickness of the Bourdon element

R - radius of curvature of the Bourdon element

μ - angle describing the length of the Bourdon tube

l - circumference of the Bourdon tube

ρ - radius of curvature of the cross-section of the Bourdon tube

ϕ - angle describing the position of a point on the circumference of the Bourdon element

k - complete modulus of elliptic functions

K - complete elliptic integral of the first kind

E - complete elliptic integral of the second kind

E^l - Young's modulus

E_l - elastic modulus from the theory of thin shells
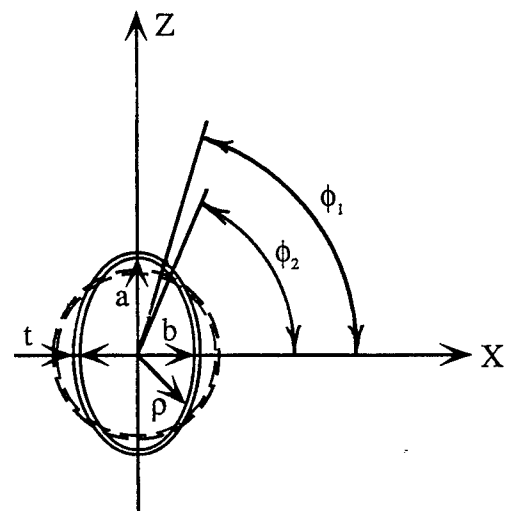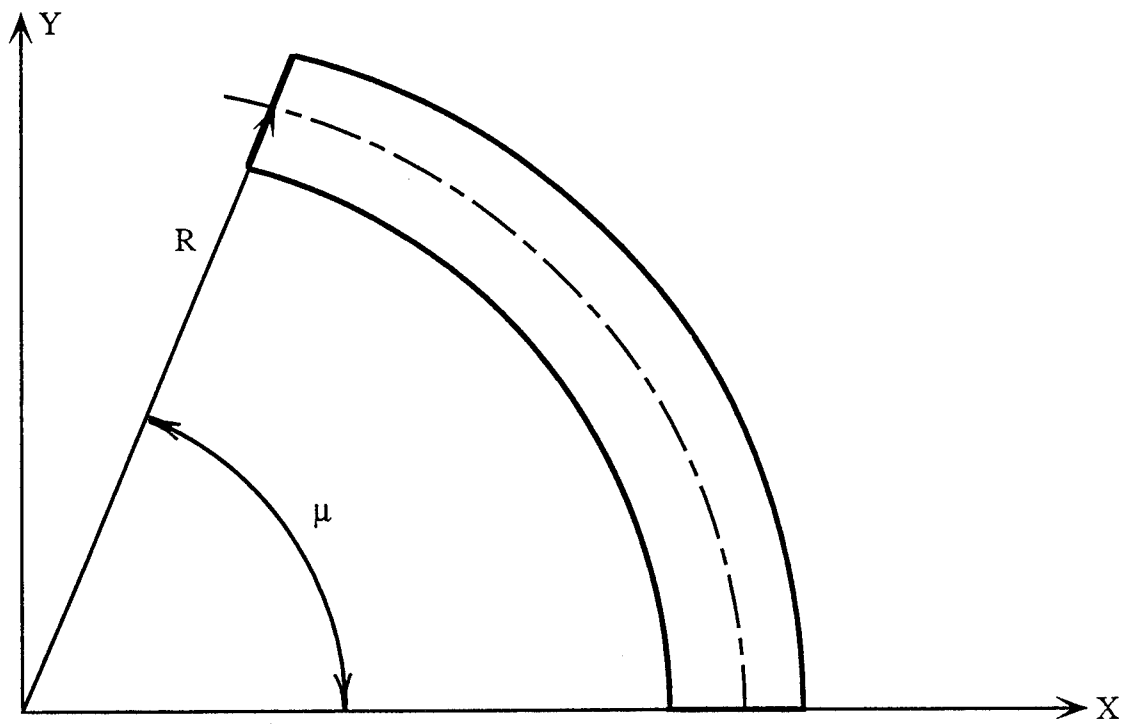
Figure 4. Bourdon length segment and cross-sectional view

2. Assumptions

In the process of developing this analytical model for Bourdon behavior, the following general assumptions were made:

a) the circumference l remains constant during cross-sectional deformation,

b) the length of the tube, defined as μR, remains constant as the elastic element straightens,

c) the wall thickness t remains constant as the cross-section changes,

d) the change in the angle ϕ ($\phi_1 - \phi_2$) is so small for small deformations that ϕ essentially remains constant during deformation, and

e) the material of the elastic element is homogeneous and isotropic.

B. MATHEMATICAL BACKGROUND

As a preface to this section, detailed derivations of all equations are presented in Appendices A-D. For the sake of clarity and brevity, only simplified expressions are presented in the body of this paper.

Some background concerning Jacobian elliptic functions and integrals is necessary for following the mathematical progression in this thesis. The following definitions

$$K = \int_0^{\frac{\pi}{2}} \frac{1}{\sqrt{1 - k^2 \cdot \sin^2 \cdot \phi}} \, d\phi \qquad\qquad 2.1$$

15

and

$$E = \int_0^{\frac{\pi}{2}} \sqrt{1 - k^2 \cdot \sin^2 \phi} \; d\phi \qquad\qquad 2.2$$

are complete elliptic integrals of the first and second kind, respectively, [Ref. 9, 10] and appear frequently throughout the problem formulation. The variable k, defined by the expression

$$k^2 = 1 - \frac{b^2}{a^2} \qquad\qquad 2.3$$

on the interval $0 \le k \le 1$, is known as the modulus of the Jacobian elliptic functions. Identities containing the elliptic functions *sn(u)*, *cn(u)*, and *dn(u)* are presented in equations 2.4.a - 2.4.f which reduce to the trigonometric functions *sin(u)*, *cos(u)*, and 1 when k is zero. Elliptic function identities relevant to this problem formulation are:

$$sn^2(u) + cn^2(u) = 1 \qquad\qquad 2.4.a$$

$$dn^2(u) + k^2 \cdot sn^2(u) = 1 \qquad\qquad 2.4.b$$

$$sn(0) = 0 \qquad\qquad 2.4.c$$

$$cn(0) = 1 \qquad\qquad 2.4.d$$

16

$$dn(0) = 1 \qquad\qquad 2.4.e$$

$$cn(K) = 0 \qquad\qquad 2.4.f$$

which are also defined in Refs. 9 and 10. Solutions for the following specific integrals are derived here for later use in the computation of strain energy in elastic Bourdon elements due to cross-sectional deformation:

$$\int_0^K dn^{-4}(u)\ du = \frac{1}{3\cdot(1-k^2)}\cdot\left[\frac{2\cdot E\cdot(2-k^2)}{(1-k^2)} - K\right] \qquad\qquad 2.5$$

$$\int_0^K dn^{-6}(u)\ du = \frac{4\cdot(2-k^2)}{15\cdot(1-k^2)^2}\cdot\left[\frac{2\cdot E\cdot(2-k^2)}{(1-k^2)} - K\right] - \frac{3\cdot E}{5\cdot(1-k^2)^2} \qquad\qquad 2.6$$

$$\int_0^K dn^{-8}(u)\ du = \left[\frac{24\cdot(2-k^2)^2}{105\cdot(1-k^2)^3} - \frac{5}{21\cdot(1-k^2)^2}\right]\cdot\left[\frac{2\cdot E\cdot(2-k^2)}{(1-k^2)} - K\right] - \frac{18\cdot E\cdot(2-k^2)}{35\cdot(1-k^2)^3}$$

$$2.7$$

17

C. PROBLEM FORMULATION

1. Geometric Relationships

Assuming that the volume of the Bourdon changes as deformation occurs, the change in the semi-major axis da is expressed as a function of the change in the semi-minor axis db by the equation

$$da = \frac{a \cdot b \cdot (E - K)}{E \cdot a^2 - K \cdot b^2} \cdot db \qquad 2.8$$

The derivation of equation 2.8 is presented in Appendix A. For a unit length, the volume of the Bourdon is defined by the equation

$$V = \pi \cdot a \cdot b \qquad 2.9$$

The change in volume then becomes

$$dV = \pi (a \cdot db + b \cdot da) \qquad 2.10$$

or

$$dV = \pi a \left[\frac{\left(a^2 + b^2\right) \cdot E - 2Kb^2}{Ea^2 - Kb^2} \right] \cdot db \qquad 2.11$$

by making the substitution for da in equation 2.10.

Bourdon tip travel is a function of the sectional deformation that occurs as a result of pressurization. For an applied internal pressure, a curved circular tube will not

straighten. But a Bourdon straightens as its elliptical cross-section becomes more circular. Because of this behavior, it is important to understand how the radius of curvature of the cross-section, ρ, changes. As can be seen in Figure 4, the radius of curvature for a circular section is constant but changes as a function of the angle ϕ for an elliptical section. A simplifying assumption here is that, as a point is mapped from the elliptical shape to the more circular shape, the defining angle ϕ is approximately the same before (ϕ_1) and after (ϕ_2) deformation for small tip travel and minimal sectional deformation.

Whereas ρ defines the radius of curvature, $1/\rho$ defines the curvature of the cross-section. The simplified expression for curvature may be written as

$$\frac{1}{\rho} = \left[\frac{b}{a^2 \cdot (1 - k^2 \cdot \sin^2 \phi)^{1.5}} \right] \qquad 2.12$$

The change in curvature, determined by taking the derivative of $1/\rho$ only with respect to dimensions a and b, is defined by the expression

$$d\left(\frac{1}{\rho}\right) = \frac{-b^2}{a^2 \cdot (1 - k^2 \cdot \sin^2 \phi)^{2.5} \cdot (Ea^2 - Kb^2)} \cdot \left[\left[\frac{(-a^2 - b^2) \cdot E}{b^2} - K \right] \cdot (1 - k^2 \cdot \sin^2 \phi) + 3 \cdot E \right] db$$

$$2.13$$

The derivative of $1/\rho$ was not taken with respect to the angle ϕ because, as stated earlier in the assumptions, ϕ is assumed to remain constant throughout pressurization and subsequent deformation.

2. Incremental Strain Energy Due to Cross-Sectional Deformation

Having derived the fundamental geometric relationships necessary to develop the analytical model, energy methods were applied to obtain a solution to the problem. In general, the elastic strain energy U in a beam due to bending is written as

$$U = \int_0^L \frac{M^2}{2 \cdot E_1 \cdot I} \, dx$$

2.14

as defined in Ref. 11. For an initially curved beam, the bending moment M is defined as

$$M = E_1 \cdot I \cdot d\left(\frac{1}{\rho}\right)$$

2.15

Figure 4 shows that, for an incremental slice of the cross-section, the wall of the tube can be modeled as a curved beam where $d(1/\rho)$ is the change in curvature of the cross-section. From the theory of thin shells, the effective elastic modulus E_1 is defined by the expression

$$E_1 = \frac{E^1}{1 - \nu^2}$$

2.16

where E^1 is the elastic modulus of a straight beam. The area moment of inertia I is defined for a unit length slice of the tube by the expression

$$I = \frac{t^3}{12}$$

2.17

Rewriting the strain energy equation as symmetric in four quadrants, the expression for the total incremental strain energy due to cross-sectional deformation is

$$dU_{xs} = 4 \cdot \int_{\bullet}^{\bullet} \frac{M^2}{2 \cdot E_1 \cdot I} \, ds \qquad 2.18$$

Substituting equations 2.15, 2.16, and A.14 into equation 2.18, the incremental strain energy becomes

$$dU_{xs} = \frac{2 \cdot E^1 \cdot I}{1 - v^2} \cdot \int_0^{\frac{\pi}{2}} a \cdot \left(d\left(\frac{1}{\rho}\right) \right)^2 \cdot \sqrt{1 - k^2 \cdot \sin^2 \phi} \; d\phi \qquad 2.19$$

and eventually, after considerable simplification,

$$dU_{xs} = \frac{2 \cdot a \cdot E^1 \cdot I \cdot C_1 \cdot db^2}{\left(1 - v^2\right)} \cdot \int_0^K \left[C_2 \cdot dn^{-4}(u) + C_3 \cdot dn^{-6}(u) + C_4 \cdot dn^{-8}(u) \right] du$$

$$2.20$$

where the constants C_1 through C_4 are defined as follows:

$$C_1 = \frac{b^4}{a^4 \cdot (Ea^2 - Kb^2)^2} \qquad 2.20.a$$

21

$$C_2 = \left(\frac{-a^2 - b^2}{b^2} \cdot E - K \right)^2 \qquad\qquad 2.20.b$$

$$C_3 = 6 \cdot E \cdot \left(\frac{-a^2 - b^2}{b^2} \cdot E - K \right) \qquad\qquad 2.20.c$$

$$C_4 = 9 \cdot E^2 \qquad\qquad 2.20.d$$

The variables K and E represent the complete elliptic integrals of the first and second kind, respectively, and are defined in equations 2.1 and 2.2. The integrals of $dn^{-4}(u)$, $dn^{-6}(u)$, and $dn^{-8}(u)$ are defined by equations 2.5, 2.6, and 2.7, respectively.

3 Incremental Strain Energy Due to Bending

To determine Bourdon incremental strain energy due to bending, or straightening in this case, an expression was developed for the total bending moment due to an applied internal pressure. Referring to Figure 5, the net moment M is found by summing the moments acting on the end cap and walls of the tube about point O. The details of this derivation are shown in Appendix C and the resulting expression is

$$\vec{M} = -P \cdot a \cdot R \cdot D \cdot (1 - \cos\beta) \cdot k \qquad\qquad 2.21$$

where P is the applied pressure, R is the radius of curvature measured to the centerline of the tube, and D is a constant for specified dimensions a and b defined as

22
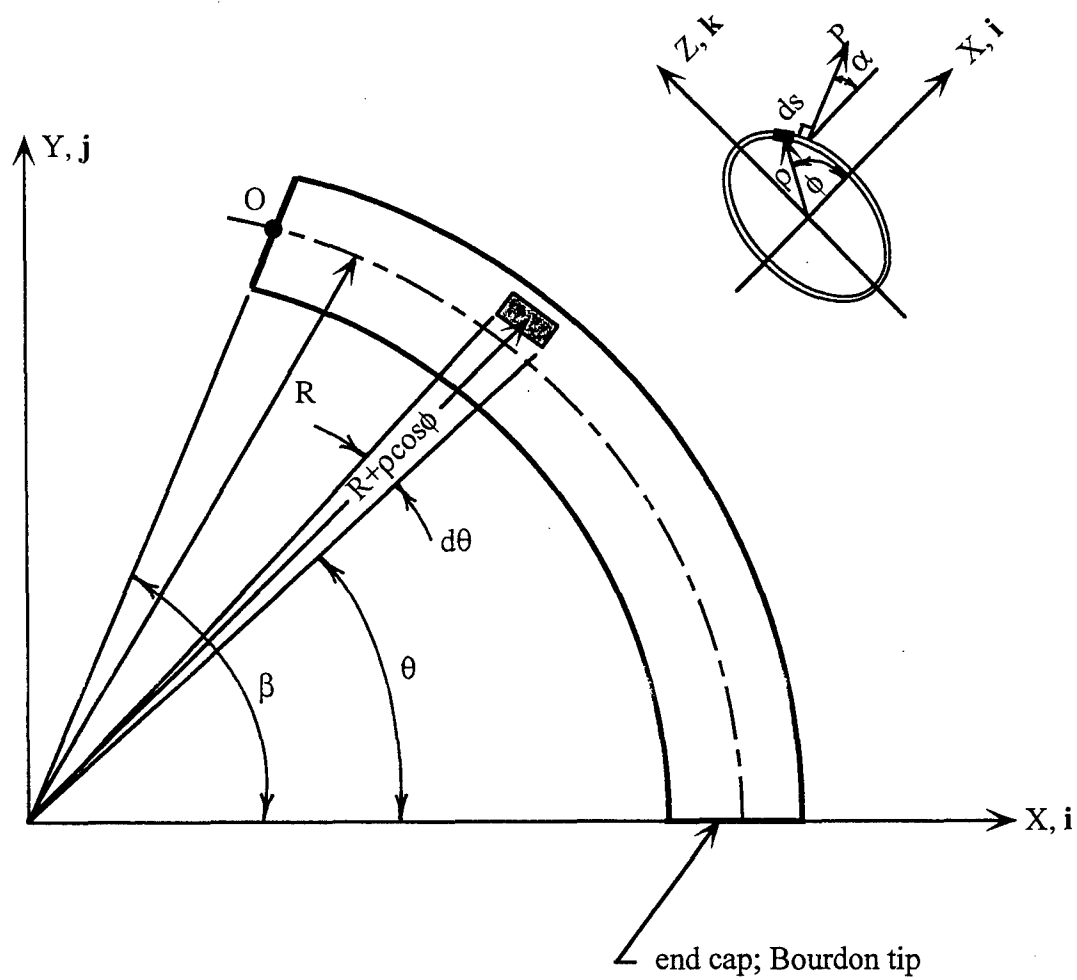
Figure 5. Bourdon length segment and cross-sectional view depicting the elemental area

for the derivation of the net moment acting on the elastic element

$$D = a\left[\frac{4}{3}\cdot\left[\frac{K-E}{k^2} + (2\cdot E - K)\right] + \pi\cdot\frac{b}{a}\right]$$

2.22

Again, K and E represent complete elliptic integrals of the first and second kind, respectively, as defined in equations 2.1 and 2.2. Substituting equations 2.21 into equation 2.14, the total strain energy due to bending of a length of tube that subtends the angle μ with the center of curvature becomes

$$U_b = \int_0^\mu \frac{(-P\cdot a\cdot R\cdot D\cdot(1 - \cos(\beta)))^2}{2\cdot E^1\cdot I}\cdot R\, d\beta$$

2.23

where the moment of inertia I is now defined as

$$I = \frac{\pi}{4}\cdot((a+t)\cdot(b+t)^3 - a\cdot b^3)$$

2.24

The incremental strain energy due to bending was found by differentiating U_b with respect to a, b, P, and R as follows:

$$dU_b = \frac{d}{da}U_b + \frac{d}{db}U_b + \frac{d}{dP}U_b + \frac{d}{dR}U_b$$

2.25

To simplify the results of this lengthy equation, the incremental strain energy due to bending is rewritten as

24

$$dU_b = A \cdot (B + Z)$$
<div align="right">2.26</div>

where A, B, and Z are defined as follows:

$$A = \frac{P \cdot a^2 \cdot R^2 \cdot D}{4 \cdot E^1 \cdot I} \cdot (6 \cdot \mu - 8 \cdot \sin(\mu) + \sin(2 \cdot \mu))$$
<div align="right">2.26.a</div>

$$B = \frac{P \cdot R \cdot b \cdot (E - K)}{(Ea^2 - Kb^2)} \cdot \left(a \cdot \frac{d}{da} D + D \right) \cdot db + P \cdot R \cdot \left(\frac{d}{db} D \right) \cdot db$$
<div align="right">2.26.b</div>

and

$$Z = (R \cdot P \cdot dP) + (1.5 \cdot P \cdot D \cdot dR)$$
<div align="right">2.26.c</div>

According to the principle of virtual work defined in Ref. 11, the change in external work is equal to the change in elastic strain energy ($dW = dU$) if a configuration satisfies geometric constraints and remains continuous. Assuming that the Bourdon satisfies these conditions,

$$dW = dU_{xs} + dU_b$$
<div align="right">2.27</div>

where the incremental external work acting on the tube is defined as

$$dW = P \cdot dV$$
<div align="right">2.28</div>

or

<div align="center">25</div>

$$(P + dP) \cdot dV = dU_{xs} + dU_b \qquad 2.29$$

Making the appropriate substitutions into equation 2.29, the resulting equation is written as

$$(P + dP) \cdot \pi \cdot a \cdot \frac{(a^2 + b^2) \cdot E - 2 \cdot K \cdot b^2}{E \cdot a^2 - K \cdot b^2} \cdot db =$$

$$\frac{2 \cdot a \cdot E^1 \cdot I \cdot C_1 \cdot db^2}{1 - \nu^2} \cdot \int_0^K \left(C_2 \cdot dn^{-4} \cdot u + C_3 \cdot dn^{-6} \cdot u + C_4 \cdot dn^{-8} \cdot u \right) du +$$

$$\frac{P \cdot a^2 \cdot R \cdot D}{4 \cdot E^1 \cdot I} \cdot (1 - \nu^2) \cdot (6 \cdot \mu - 8 \cdot \sin\mu + \sin(2 \cdot \mu)) \times$$

$$\left[\frac{P \cdot R \cdot b \cdot (E - K)}{(E \cdot a^2 - K \cdot b^2)} \left(a \cdot \frac{d}{da} D + D \right) \cdot db + P \cdot R \cdot \left(\frac{d}{db} D \right) \cdot db + P \cdot R \cdot dP + \frac{3 \cdot P \cdot D}{2} \cdot dR \right]$$

$$2.30$$

which is quadratic in *db* where *dR* is also unknown. See Appendix B for derivation details.

4. Tip Travel

The equation for tip travel was derived by making the assumption that the length of the Bourdon remains constant for any given pressure and by applying Castigliano's second theorem. The assumption for constant length, L, written as

$$\mu \cdot R = L \qquad\qquad 2.31$$

implies that

$$\mu \cdot dR + R \cdot d\mu = 0 \qquad\qquad 2.32$$

or that incremental tip travel dR can be calculated using the expression

$$dR = \frac{-R \cdot d\mu}{\mu} \qquad\qquad 2.33$$

Whereas R and μ are known quantities, the variable $d\mu$ is undefined. Referring to

Figure 6,

$$d\mu = -\theta_i \qquad\qquad 2.34$$

by geometry where θ_i , the angle of rotation of the tip due to the applied dummy moment,

is described by the equation

$$\theta_i = \int_0^L \frac{M}{E^1 \cdot I} \cdot \left(\frac{d}{dM_i} M\right) dx \qquad\qquad 2.35$$

which is the application of Castigliano's second theorem [Ref.11]. When the dummy

moment, M_i is applied, the equation for the net moment becomes

$$\vec{M} = -P \cdot a \cdot R \cdot D \cdot (1 - \cos\beta) \cdot k - M_i \cdot k \qquad\qquad 2.36$$

27
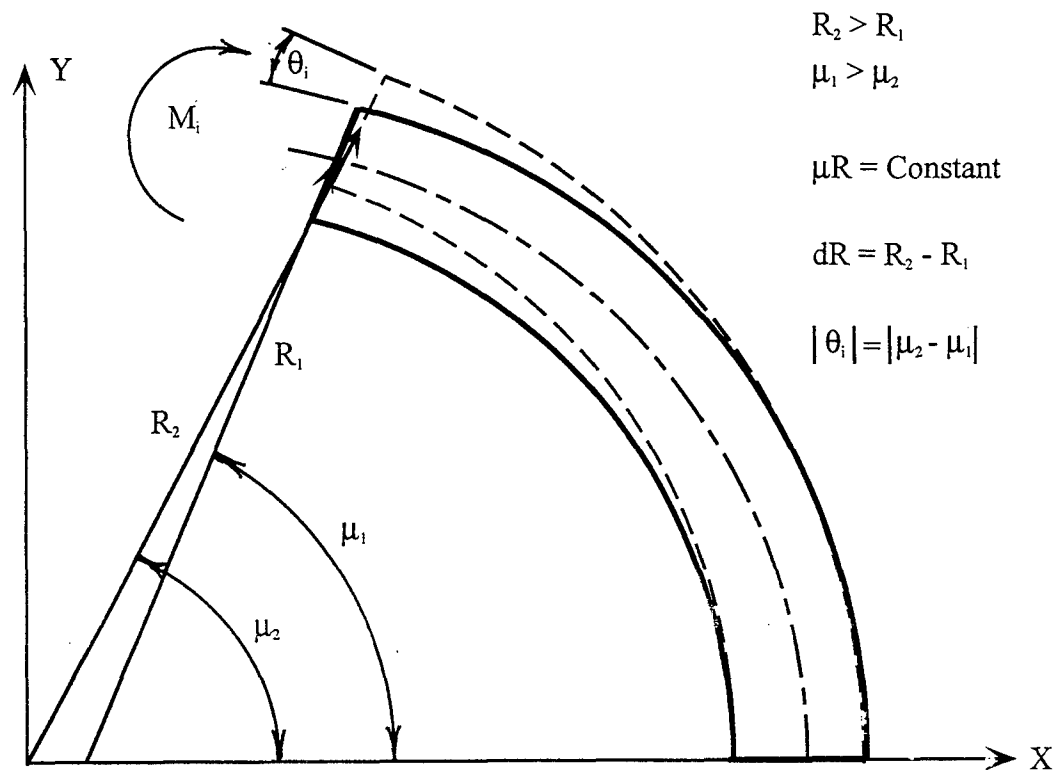
Figure 6. Bourdon length segment and tip deflection for the application of

Castigliano's second theorem

Substituting equation 2.36 into equation 2.35 and setting the dummy moment equal to zero, the expression for tip rotation is obtained by integrating

$$\theta_i = \frac{P \cdot a \cdot R \cdot D}{E^l \cdot I} \cdot (\mu - sin\mu)$$

2.37

In this formulation, tip displacement is calculated iteratively. For this model, knowing θ_i defines $d\mu$ which then allows the determination of incremental tip travel dR. Once dR is known, db is found by solving equation 2.29 and da is calculated using equation 2.8. Subsequent values of dR are then calculated using incremented values of a and b.

D. SIMULATION PROGRAM AND ANALYTICAL RESULTS

1. Source Code Description and Limitations

Considerable effort was expended in expressing all of the equations in Chapter II as functions of a, b, k, E, and K to simplify the programming portion of this research effort. Having derived the requisite equations to determine tip travel and sectional deformation, a program was written in FORTRAN to iteratively calculate solutions for user-defined Bourdon properties, geometries, and operating pressures. The source code, listed in Appendix E, defines all program variables, prompts the user for input, and then calls seven subroutines to iteratively calculate tip travel and corresponding changes in tip geometry.

The topics of temperature effects and the standard methods of compensation discussed in Chapter I were not addressed in this attempt to develop an analytical

29

solution for Bourdon tip displacement. The analytical model presented in this paper only calculates tip travel and cross-sectional deformation as functions of pressure.

2. Analytical Results

Execution of the source code *Program Bourdon* was very sensitive to the geometric relationships between a, b, and R and worked best for $a{:}b$ ratios near 2:1 and for $0 < R < 34$ mm $(0 < R < 1.34$ in). The program ceased to work beyond one iteration once R exceeded 33 mm.

The following table indicates analytical results for fictitious Bourdon elements each fabricated from phosphor bronze having an elastic modulus of 110 GPa $(16 \times 10^6$ psi) and a Poisson's ratio of 0.34:

Table 1. Analytical Solutions Generated from *Program Bourdon*

Bourdon Element	Major Axis (2a) [mm/in]	Minor Axis (2b) [mm/in]	Radius of Curvature (R) [mm/in]	Wall Thickness (t) [mm/in]	Angle Describing Tube Length (μ) [deg/rad]	Max. Applied Pressure (P) [MPa/psi]	Tip Travel (dR) [mm/in]
1	10.000 / 0.393	5.000 / 0.197	30.000 / 1.181	0.300 / 0.012	250 / 4.363	1.00 / 145.00	1.54 / 0.06
2	10.000 / 0.393	5.000 / 0.197	30.000 / 1.181	0.100 / 0.004	250 / 4.363	1.00 / 145.00	41.54 / 1.64
3	10.0 / 0.393	5.000 / 0.197	30.000 / 1.181	0.300 / 0.012	330 / 5.760	1.00 / 145.00	1.38 / 0.05
4	10.0 / 0.393	5.000 / 0.197	20.000 / 0.787	0.300 / 0.012	250 / 4.363	1.00 / 145.00	0.46 / 0.02

5	10.0 / 0.393	5.000 / 0.197	50.000 / 1.97	0.300 / 0.012	250 / 4.363	1.00 / 145.00	7.12 / 0.28
6	14.000 / 0.551	5.000 / 0.197	30.000 / 1.181	0.100 / 0.004	250 / 4.363	1.00 / 145.00	112.41 / 4.43
7	14.000 / 0.551	5.000 / 0.197	20.000 / 0.787	0.100 / 0.004	250 / 4.363	1.00 / 145.00	33.31 / 1.31
8	7.500 / 0.295	5.000 / 0.197	20.000 / 0.787	0.100 / 0.004	250 / 4.363	1.00 / 145.00	4.32 / 0.17
9	7.500 / 0.295	5.000 / 0.197	30.000 / 1.181	0.100 / 0.004	250 / 4.363	1.00 / 145.00	14.57 / 0.57

Looking at the results of the analytical model, some of the tip deflections are excessively large while others are of more reasonable magnitudes. These extremes in output are currently unexplained and under investigation. While the validity of the analytical model's results is unknown, an important observation is made concerning the trends of the output. As stated previously in Chapter I, Bourdon elements having flatter cross-sections and thinner walls exhibit larger tip displacements than rounder, thicker elements for the same applied pressure. The results presented in Table 1 show trends that agree with Bourdon displacement theory.

Comparing Bourdon elements 1 and 2 from Table 1, element 2 has a thinner wall than element 1 and consequently experiences significantly more tip travel. Looking at the major axes of elements 2, 6, and 9, element 6 has the flattest cross-section followed, in increasing order, by elements 2 and 9, respectively. As expected, element 6 exhibits

31

the greatest tip movement and element 9 exhibits the least when all other parameters are held constant between the three specified elements. Similar comparisons can also be made between other elements in Table 1.

III. EXPERIMENTAL AND NUMERICAL ANALYSES OF A BOURDON TUBE

A. EXPERIMENTAL ANALYSIS

Because analytical studies are based on assumptions, it is good practice to compare analytical results with experimental data. Doing so verifies the validity of the mathematical model and its underlying assumptions. For the model developed in this thesis, a good correlation between analytical results and experimental data implies the successful application of this analytical model to future designs of Bourdon gauges.

The experimental results presented in Tables 2 and 3 were obtained by two naval facilities: the calibration laboratory at the Regional Repair Center (RRC), Norfolk, and the Mechanical Instrument Repair Calibration Shop (MIRCS) in USS SHENANDOAH (AD-44), homeported in Norfolk. The requested information was faxed to SIMA, Norfolk and was then disseminated to the aforementioned facilities. Pertinent dimensions, elastic element information, and Bourdon tip travel results from the experimental studies are:

33

Table 2. Experimental Data from RRC

Gauge Company and Range [psi]	Bourdon Material	Major Axis (2a) [in/mm]	Minor Axis (2b) [in/mm]	Radius of Curvature (R) [in/mm]	Applied Pressure (P) [psi/MPa]	Tip Travel (dR) [in/mm]
Weksler 0-300	**Alloy Steel**	0.5737 / 14.5720	0.2220 / 5.6388	1.361 / 34.5694	300.00 / 2.07	0.25 / 6.35
Mensor 0-1000	**Stainless Steel**	0.5559 / 14.1199	0.2936 / 7.4574	3.0843 / 78.3412	1000.00 / 6.89	0.4375 / 11.1125
Heise 0-3000	**Stainless Steel**	0.4108 / 10.4343	0.2758 / 7.0053	3.5129 / 89.2277	3000.00 / 20.68	0.25 / 6.35

Table 3. Experimental Data from MIRCS

Bourdon Material	Major Axis (2a) [in/mm]	Minor Axis (2b) [in/mm]	Radius of Curvature (R) [in/mm]	Applied Pressure (P) [psi/MPa]	Tip Travel (dR) [in/mm]
Stainless Steel	0.5 / 12.7	0.115 / 2.921	0.771 / 19.571	500 / 3.45	0.131 / 3.327
Beryllium Copper	0.5 / 12.7	0.190 / 4.826	1.033 / 26.236	600 / 4.14	0.129 / 3.277

One key parameter missing from Tables 2 and 3 is the Bourdon wall thickness of each gauge. Whereas the major and minor diameters were easily measured, wall thicknesses were neither measurable nor available from the respective manufacturers due to the proprietary nature of the information.

34

B. FINITE ELEMENT ANALYSIS

One rapidly growing approach to engineering problem solving is the numerical technique of finite element analysis. These techniques (1) discretize a domain with a finite number of finite elements and a finite number of nodes per element, (2) introduce nodal points and appropriate shape functions to represent the trial solution in each element, and (3) transform the resulting set of differential equations into a series of matrix equations to change a system from an infinite degree of freedom system to a finite degree of freedom system of appropriate size.

Several powerful finite element software packages exist today that compute solutions for complicated engineering problems. For the purpose of this research, the ability to build, constrain, and pressurize a Bourdon tube using computer graphics greatly enhanced the study of Bourdon behavior. As powerful as this tool can be, however, this type of analysis did not preclude the effort to conduct laboratory experiments but rather supplemented the study of Bourdon behavior. Once the models were constructed and drawn to match the dimensions and material properties of the Bourdons used in the experimental studies, tip displacement results were quickly determined.

The finite element solutions presented in this paper were generated using I-DEAS Simulation software, software that builds geometry and finite element models, analyzes the models, and evaluate the results. Each of the finite element models presented in this paper was constructed using the following parameters: (1) major axis $2a$, (2) minor axis $2b$, (3) wall thickness t, (4) radius of curvature R, (5) Bourdon arc length μ, (6) elastic modulus E, (7) Poisson's ratio v, and (8) applied pressure P.

35

Assumptions for wall thickness and arc length were made based on design information presented in Refs. 1 and 5. Boundary conditions were applied at one end of each Bourdon model. The socket or pressure end was clamped to prevent rotation and translation in the x, y, and z directions. The tip end of each model was sealed but otherwise left unconstrained to allow maximum freedom of movement. Internal pressures corresponding to experimental test pressures were applied to the walls and end cap (tip) of each finite element model.

The numerical models were analyzed using linear, thin-shelled elements whose thicknesses were modified to match the estimated wall thicknesses of the Bourdon elements listed in Table 1. The quality of the mesh for each element was established using criteria for distortion. On a scale of -1.0 to 1.0, an element is perfectly square for a distortion value of 1.0. Meshes exhibiting distortion values less than zero are very bad and should be avoided whereas distortion values greater than 0.4 are acceptable. In modeling the Bourdon elements using I-DEAS, all of the meshes exhibited distortion levels greater than 0.4. The elements that were distorted, however, consistently occurred along the length of the element at the major axis.

The following table summarizes numerical solutions for tip displacement in Bourdon elements having the same geometries and material properties as those presented in ChapterII,Table 1:

Table 4. Numerical Solutions for Table 1 Bourdons

Bourdon Element	Major Axis (2a) [mm/in]	Minor Axis (2b) [mm/in]	Radius of Curvature (R) [mm/in]	Wall Thickness (t) [mm/in]	Angle Describing Tube Length (μ) [deg/rad]	Max. Applied Pressure (P) [MPa/psi]	Tip Travel (dR) [mm/in]
1	10.000/ 0.393	5.000 / 0.197	30.000 / 1.181	0.300 / 0.012	250 / 4.363	1.00 / 145.00	3.26 / 0.13
7	14.000 / 0.551	5.000 / 0.197	20.000 / 0.787	0.100 / 0.004	250 / 4.363	1.00 / 145.00	42.8 / 1.69
8	7.500 / 0.295	5.000 / 0.197	20.000 / 0.787	0.100 / 0.004	250 / 4.363	1.00 / 145.00	8.50 / 0.33

Bourdon elements 1, 7, and 8 were chosen from Table 1 at random for modeling in I-DEAS. As for the case of the analytical model, the validity of the magnitudes of tip deflection generated by the finite element technique is also uncertain without comparative data from gauge manufacturers or more extensive experimental work.

Comparing the results from Tables 1 and 4, the numerical solutions follow the same trends as those from the analytical model but at greater magnitudes of tip deflection. Tip travel is 53%, 22%, and 49% greater for I-DEAS elements 1, 7, and 8, respectively, than for the same analytical elements in Table 1.

IV. CONCLUSIONS AND RECOMMENDATIONS

A. CONCLUSIONS

The objective to analytically derive a model to predict Bourdon behavior was a very challenging one. The very mechanism by which Bourdons move, as described in Chapter I, indicates the level of complexity of this engineering problem. The simple beam and thin-shell theories and equations used in the development of this analytical model for tip travel in a Bourdon tube have produced solutions whose validity is yet to be determined.

The task of comparing analytical, numerical, and experimental results was hampered by insufficient experimental data, questionable numerical solutions, and forced assumptions concerning Bourdon geometry and material. The fact that *Program Bourdon* produced output that followed expected trends is encouraging. The fact that the code runs for more than one iteration only for certain Bourdon geometries warrants continued investigation.

The experimental data collected from RRC and MIRCS was very limited due, in some part, to the underspecification of the requested information. Ideally, the dimensions of the elastic elements should have come from the gauge manufacturers, but as stated previously, that information is closely guarded by the companies that design and manufacture the gauges. In addition, the tip travel for each bourdon element should have been measured over the operating range of the gauge and not just at the maximum allowable pressure.

The accuracy of the numerical results generated in I-DEAS was questionable due to the excessive magnitudes of tip deflection for the applied pressures. Because the experimental and numerical results for tip travel were each somewhat inconclusive and because the analytical results were constrained by the geometric relationships of dimensions a, b, and R, the comparative study of results yielded little useful information for us to be able to state with conviction the accuracy of the analytical results. Consequently, the validity of the analytical model remains under investigation.

B. RECOMMENDATIONS FOR FUTURE RESEARCH

The research results presented in this paper are rather limited implying that a considerable amount of work still needs to be done to develop an acceptable analytical model for Bourdon behavior. The following suggestions are made to continue the research effort:

1. Peruse Chapter VII (*Tubular Manometric Springs*) of Ref. 12 for its detailed discussion of Bourdon tubes and compare the assumptions and derivations presented in this thesis to the theories presented in *Elastic Elements of Instruments*. This book is highly recommended by the Heise Division of Dresser Instruments as an excellent resource in developing an analytical model for Bourdon behavior.

2. As a means of eliminating the geometric constraints of the analytical model, modify the model using less restrictive geometric assumptions by independently considering variable Bourdon length, circumference, and angle ϕ.

3. Collect more thorough experimental data covering a much broader operational range of pressures to better analyze and predict Bourdon behavior and eliminate as many assumptions as possible concerning Bourdon geometry by obtaining comprehensive measurements.

4. Enhance the analytical model to include a stress analysis to predict failure from fatigue due to cyclic loading or from overpressurization and exploit the ability of finite element software packages to calculate stresses and strains within finite element models for comparison purposes.

APPENDIX A. GEOMETRIC RELATIONSHIPS

Geometric relationships are derived in great detail in this appendix. These relationships ultimately serve as the building blocks for the formulation of the analytical model for Bourdon behavior. Derivations for da, the change in the semi-major axis, dV, the volumetric change of the tube of unit length, and $d(1/\rho)$, the change in the curvature of the cross-section, are presented in this appendix.

Referring to Figure 4, the equation for the elliptical cross-section is

$$\frac{x^2}{b^2} + \frac{z^2}{a^2} = 1 \qquad\qquad A.1$$

and the area, A, is

$$A = \pi \cdot a \cdot b \qquad\qquad A.2$$

The volume of the elliptical tube with length unity is

$$V = \pi \cdot a \cdot b \qquad\qquad A.3$$

and the change in volume is

$$dV = \pi \cdot (a \cdot db + b \cdot da) \qquad\qquad A.4$$

The circumference, l, of an ellipse is defined as

$$l = 4 \cdot \int_0^{\frac{\pi}{2}} ds \qquad\qquad A.5$$

where ds is an incremental length of the circumference defined by the radius of curvature of the cross-section ρ and the angle ϕ. Referencing Figure 4 for small $d\phi$,

$$ds = \sqrt{dx^2 + dz^2} \qquad\qquad A.6$$

For

$$x = b \cdot \cos\phi \qquad\qquad A.7$$

and

$$z = a \cdot \sin\phi \qquad\qquad A.8$$

the following expressions are true:

$$dx^2 = b^2 \cdot \sin^2 \phi \cdot d\phi^2 \qquad\qquad A.9$$

and

$$dz^2 = a^2 \cdot \cos^2 \phi \cdot d\phi^2 \qquad\qquad A.10$$

Substituting equations A.9 and A.10 into equation A.6 and dividing both sides by the square root of a^2,

44

$$ds = a \cdot \sqrt{\frac{b^2}{a^2} \cdot \sin^2 \phi + \cos^2 \phi} \cdot d\phi \qquad \text{A.11}$$

Substituting in the trigonometric identity $cos^2 \phi = 1 - sin^2 \phi$ and rearranging terms,

$$ds = a \cdot \sqrt{\left(\frac{b^2}{a^2} - 1\right) \cdot \sin^2 \phi + 1} \cdot d\phi \qquad \text{A.12}$$

The new variable k is defined by the expression

$$k^2 = 1 - \frac{b^2}{a^2} \qquad \text{A.13}$$

on the interval $0 \le k \le 1$. The incremental arc length ds is now written as

$$ds = a \cdot \sqrt{1 - k^2 \cdot \sin^2 \phi} \cdot d\phi \qquad \text{A.14}$$

so that the circumference becomes

$$l = 4 \cdot a \cdot \int_0^{\frac{\pi}{2}} \sqrt{1 - k^2 \cdot \sin^2 \phi} \ d\phi \qquad \text{A.15}$$

and then

$$l = 4 \cdot a \cdot E \qquad \text{A.16}$$

45

where E is the complete elliptic integral of the second kind defined by equation 2.2. For the assumption that l is constant, $dl = 0$. Taking the derivative of equation A.16 and equating it to zero yields the following expression:

$$a \cdot \left[\left(\frac{d}{dk} E \right) \cdot dk \right] + E \cdot da = 0 \qquad \text{A.17}$$

Solving for dk, the derivative of both sides of equation A.14 is taken and written as

$$k \cdot dk = \frac{-b}{a^3} \cdot (a \cdot db - b \cdot da) \qquad \text{A.18}$$

then as

$$dk = \frac{b}{k \cdot a^3} \cdot (b \cdot da - a \cdot db) \qquad \text{A.19}$$

and eventually as

$$dk = \frac{b^2 \cdot da - a \cdot b \cdot db}{a^2 \cdot \sqrt{a^2 - b^2}} \qquad \text{A.20}$$

after making the substitution for k defined by equation A.13. From Ref. 9,

$$\frac{d}{dk} E = \frac{E - K}{k} \qquad \text{A.21}$$

where K is the complete elliptic integral of the first kind defined by equation 2.1.

Substituting equations A.20 and A.21 into equation A.17 yields

$$b \cdot \left(\frac{E - K}{k} \right) \cdot \left(\frac{b \cdot da - a \cdot db}{k \cdot a^2} \right) + E \cdot da = 0 \qquad \text{A.22}$$

which simplifies to

$$\frac{(E \cdot b^2 - K \cdot b^2) \cdot da + (K \cdot a \cdot b - E \cdot a \cdot b) \cdot db + (E \cdot a^2 - E \cdot b^2) \cdot da}{a^2 - b^2} = 0 \qquad \text{A.23}$$

and eventually to

$$da = \frac{a \cdot b \cdot (E - K)}{E \cdot a^2 - K \cdot b^2} \cdot db \qquad \text{A.24}$$

the ultimate expression of the change in the semi-major axis written as a function of the change in the semi-minor axis. Substituting this expression into equation A.4, the volumetric change in the Bourdon may be written as a function of db as follows:

$$dV = \pi \cdot \left[a \cdot db + b \cdot \left[\frac{a \cdot b \cdot (E - K)}{E \cdot a^2 - K \cdot b^2} \cdot db \right] \right] \qquad \text{A.25}$$

After some algebraic manipulation, the change in volume is written as

$$dV = \pi \cdot a \cdot \frac{(a^2 + b^2) \cdot E - 2 \cdot K \cdot b^2}{E \cdot a^2 - K \cdot b^2} \cdot db \qquad \text{A.26}$$

47

Referencing Figure 4, the radius of curvature ρ of the cross-section is defined by the relation

$$\rho = \frac{ds}{d\phi}$$

A.27

and the curvature is defined by the expression

$$\frac{1}{\rho} = \frac{\dfrac{d^2 \cdot z}{dx^2}}{\left[1 + \left(\dfrac{dz}{dx}\right)^2\right]^{1.5}}$$

A.28

The objective now is to write curvature as a function of the parameters a, b, and ϕ. Recalling equation A.1, its derivative is

$$\frac{x \cdot dx}{b^2} + \frac{z \cdot dz}{a^2} = 0$$

A.29

Solving for dz/dx,

$$\frac{dz}{dx} = \frac{-a^2 \cdot x}{b^2 \cdot z}$$

A.30

so that

$$\left(\frac{dz}{dx}\right)^2 = \frac{a^4 \cdot x^2}{b^4 \cdot z^2}$$

A.31

The next objective is to write dz^2/dx^2 in terms of a, b, and ϕ. By definition,

48

$$\frac{d^2 \cdot z}{dx^2} = \frac{d}{dx} \left(\frac{dz}{dx} \right)$$ A.32

With the substitution of equation A.30, equation A.32 becomes

$$\frac{d^2 \cdot z}{dx^2} = \frac{d}{dx} \cdot \left(\frac{-a^2 \cdot x}{b^2 \cdot z} \right)$$ A.33

or

$$\frac{d^2 \cdot z}{dx^2} = \frac{-a^2}{b^2} \cdot \frac{d}{dx} \cdot \left(\frac{x}{z} \right)$$ A.34

which, when the derivative is taken, becomes

$$\frac{d^2 \cdot z}{dx^2} = \frac{-a^2}{b^2} \cdot \left[\frac{(z \cdot 1) - \left(x \cdot \frac{dz}{dx} \right)}{z^2} \right]$$ A.35

Substituting equation A.30 into equation A.35 and simplifying, equation A.35 may be rewritten as

$$\frac{d^2 \cdot z}{dx^2} = \frac{-a^2}{b^2 \cdot z} \cdot \left[1 - \frac{x}{z} \cdot \left(\frac{-a^2 \cdot x}{b^2 \cdot z} \right) \right]$$ A.36

and eventually as

49

$$\frac{d^2 z}{dx^2} = \frac{-a^4}{b^2 \cdot z^3}$$

A.37

Now substituting equations A.30 and A.37 into equation A.28, curvature is expressed as

$$\frac{1}{\rho} = \frac{-a^4}{b^2 \cdot z^3} \cdot \frac{1}{\left(1 + \frac{a^4 \cdot x^2}{b^4 \cdot z^2}\right)^{1.5}}$$

A.38

which, after a few algebraic manipulations, becomes

$$\frac{1}{\rho} = \frac{-a^4 \cdot b^4}{\left(b^4 \cdot z^2 + a^4 \cdot x^2\right)^{1.5}}$$

A.39

Substituting equations A.9 and A.10 into equation A.39, curvature is written as

$$\frac{1}{\rho} = \frac{-a^4 \cdot b^4}{\left(b^4 \cdot a^2 \cdot \sin^2 \phi + a^4 \cdot b^2 \cdot \cos^2 \phi\right)^{1.5}}$$

A.40

or as

$$\frac{1}{\rho} = \frac{-a \cdot b}{\left(b^2 \cdot \sin^2 \phi + a^2 \cdot \cos^2 \phi\right)^{1.5}}$$

A.41

Recalling the trigonometric identity $cos^2\phi = 1 - sin^2\phi$, and dividing the numerator and denominator by a^3,

50

$$\frac{1}{\rho} = \frac{-b}{\left[\frac{b^2}{a^2} \cdot \sin^2 \phi + (1 - \sin^2 \phi)\right]^{1.5} \cdot a^2} \qquad \text{A.42}$$

and ultimately

$$\frac{1}{\rho} = \frac{-b}{a^2 \cdot (1 - k^2 \cdot \sin^2 \phi)^{1.5}} \qquad \text{A.43}$$

Considering the absolute value of the curvature

$$\frac{1}{\rho} = \frac{b}{a^2 \cdot (1 - k^2 \cdot \sin^2 \phi)^{1.5}} \qquad \text{A.44}$$

which now correlates to the definition of curvature for an elliptical cross-section as defined in Ref. 13. The change in curvature may now be written as

$$d \cdot \left(\frac{1}{\rho}\right) = \frac{-1}{\rho^2} \cdot d\rho \qquad \text{A.45}$$

where

$$-\frac{1}{\rho^2} = \frac{b^2}{a^4 \cdot (1 - k^2 \cdot \sin^2 \phi)^3} \qquad \text{A.46}$$

and

$$d\rho = \left(\frac{d}{da}\rho\right) \cdot da + \left(\frac{d}{db}\rho\right) \cdot db + \left(\frac{d}{dk}\rho\right) \cdot dk$$

A.47

The derivative is taken with respect to k because k is a function of the dimensions a and b as defined by equation A.13. The partial derivatives of ρ with respect to a, b, and k are

$$\left(\frac{d}{da}\rho\right) \cdot da = \frac{2 \cdot a}{b} \cdot (1 - k^2 \cdot \sin^2 \phi)^{1.5} \cdot da$$

A.47.a

$$\left(\frac{d}{db}\rho\right) \cdot db = -\frac{a^2}{b^2} \cdot (1 - k^2 \cdot \sin^2 \phi)^{1.5} \cdot db$$

A.47.b

$$\left(\frac{d}{dk}\rho\right) \cdot dk = \frac{-3 \cdot a^2 \cdot k \cdot dk \cdot \sin^2 \phi}{b} \cdot \sqrt{1 - k^2 \cdot \sin^2 \phi}$$

A.47.c

so that equation A.47 becomes

$$d\rho = \left(\frac{2 \cdot a}{b} \cdot da - \frac{a^2}{b^2} \cdot db\right) \cdot (1 - k^2 \cdot \sin^2 \phi)^{1.5} - \frac{3 \cdot a^2 \cdot k \cdot dk \cdot \sin^2 \phi}{b} \cdot \sqrt{1 - k^2 \cdot \sin^2 \phi}$$

A.48

Recalling equations A.13 and A.19, the expression kdk may be written as

$$k \cdot dk = \frac{b}{a^3} \cdot (b \cdot da - a \cdot db)$$

A.49

Making the substitutions for *da* and *kdk* and simplifying, equation A.48 becomes

$$d\rho = \frac{a^2}{b^2} \left[\frac{(2b^2 - a^2) \cdot E - Kb^2}{Ea^2 - Kb^2} \right] \cdot (1 - k^2 \cdot \sin^2 \phi)^{1.5} \cdot db -$$

$$3 \cdot E \cdot \sin^2 \phi \cdot \left(\frac{b^2 - a^2}{Ea^2 - Kb^2} \right) \cdot \sqrt{1 - k^2 \cdot \sin^2 \phi} \cdot db$$

$$A.50$$

which is even further simplified by manipulating the following terms:

$$\sin^2 \phi \cdot \sqrt{1 - k^2 \cdot \sin^2 \phi} = -\frac{1}{k^2} \cdot \sqrt{1 - k^2 \cdot \sin^2 \phi} \cdot ((1 - k^2 \cdot \sin^2 \phi) - 1) \qquad A.51$$

or

$$\sin^2 \phi \cdot \sqrt{1 - k^2 \cdot \sin^2 \phi} = -\frac{1}{k^2} \cdot \left[(1 - k^2 \cdot \sin^2 \phi)^{1.5} - \sqrt{1 - k^2 \cdot \sin^2 \phi} \right] \qquad A.52$$

Making the substitution of equations A.13 and A.52 into equation A.50 , the expression

for the change in the radius of curvature becomes

$$d\rho = \frac{3 \cdot a^2 \cdot E}{Ea^2 - Kb^2} \cdot \sqrt{1 - k^2 \cdot \sin^2 \phi} \cdot db +$$

$$\left[\frac{a^2}{b^2} \cdot \frac{(2 \cdot b^2 - a^2) \cdot E - K \cdot b^2}{Ea^2 - Kb^2} - \frac{3 \cdot a^2 \cdot E}{Ea^2 - Kb^2} \right] \cdot (1 - k^2 \cdot \sin^2 \phi)^{1.5} \cdot db$$

$$A.53$$

which, with a little more manipulation, becomes

$$d\rho = \frac{a^2}{Ea^2 - Kb^2} \cdot \left[3 \cdot E \cdot \sqrt{1 - k^2 \cdot \sin^2 \phi} - \frac{((a^2 + b^2) \cdot E + K \cdot b^2) \cdot (1 - k^2 \cdot \sin^2 \phi)^{1.5}}{b^2} \right] \cdot db$$

A.54

Now substituting equations A.46 and A.54 into equation A.45, the change in curvature is written as

$$d\left(\frac{1}{\rho}\right) = \frac{-b^2}{a^2 \cdot (1 - k^2 \cdot \sin^2 \phi)^{2.5} \cdot (Ea^2 - Kb^2)} \cdot \left[3 \cdot E - \left[\frac{(a^2 + b^2) \cdot E}{b^2} + K \right] \cdot (1 - k^2 \cdot \sin^2 \phi) \right] \cdot db$$

A.55

54

APPENDIX B. INCREMENTAL STRAIN ENERGY DUE TO CROSS-SECTIONAL DEFORMATION

In general, elastic strain energy for a beam subjected to transverse loading is expressed as

$$U = \int_0^L \frac{M^2}{2 \cdot E \cdot I} \, dx \qquad\qquad B.1$$

So as not confuse the symbols for elastic modulus and elliptic integrals of the second kind, elastic modulus for a straight beam will be designated E', elastic modulus derived from the theory of thin shells will be designated E_I, and elliptic integrals of the second kind will be designated E for all remaining calculations. For an initially curved beam, the moment M is defined by the expression

$$M = E_1 \cdot I \cdot \frac{1}{\rho} \qquad\qquad B.2$$

Incremental strain energy in the bourdon due to a change in the cross-section is written as

$$dU_{xs} = 4 \cdot \int_0^{\frac{\pi}{2}} \frac{M^2}{2 \cdot E_1 \cdot I} \, ds \qquad\qquad B.3$$

where M is now defined as

$$M = E_1 \cdot I \cdot d\left(\frac{1}{\rho}\right) \qquad \text{B.4}$$

Making the appropriate substitutions for M and E_1, equation B.3 becomes

$$dU_{xs} = \frac{2 \cdot E^1 \cdot I}{1 - \nu^2} \cdot \int_0^{\frac{\pi}{2}} \left(d\left(\frac{1}{\rho}\right)\right)^2 ds \qquad \text{B.5}$$

where, for a unit length, the area moment of inertia is defined as

$$I = \frac{t^3}{12} \qquad \text{B.6}$$

and t is the wall thickness of the Bourdon element. The integral term is found by squaring equation A.45 which results in the expression

$$\left(d\left(\frac{1}{\rho}\right)\right)^2 =$$

$$\left[\frac{-b^2}{a^3 \cdot (1 - k^2 \cdot \sin^2 \phi)^{2.5} \cdot (Ea^2 - Kb^2)} \cdot \left[3 \cdot E - \left[\frac{(a^2 + b^2) \cdot E}{b^2} + K\right] \cdot (1 - k^2 \cdot \sin^2 \phi)\right] \cdot db\right]^2$$

$$\text{B.7}$$

which upon squaring becomes

$$\left(d\left(\frac{1}{\rho}\right)\right)^2 =$$

$$\frac{b^4}{a^4 \cdot (Ea^2 - Kb^2)} \cdot \left[\frac{\left[\frac{(a^2 + b^2) \cdot E}{b^2} + K\right]^2}{(1 - k^2 \cdot \sin^2 \phi)^3} - 6 \cdot E \cdot \frac{\frac{(a^2 + b^2) \cdot E}{b^2} + K}{(1 - k^2 \cdot \sin^2 \phi)^4} + \frac{9 \cdot E^2}{(1 - k^2 \cdot \sin^2 \phi)^5} \right] \cdot db^2$$

For simplicity, equation B.8 is rewritten as

B.8

$$\left(d\left(\frac{1}{\rho}\right)\right)^2 = C_1 \cdot \left[\frac{C_2}{(1 - k^2 \cdot \sin^2 \phi)^3} + \frac{C_3}{(1 - k^2 \cdot \sin^2 \phi)^4} + \frac{C_4}{(1 - k^2 \cdot \sin^2 \phi)^5} \right] \cdot db^2$$

where the constants C_1 through C_4 are defined as follows:

B.9

$$C_1 = \frac{b^4}{a^4 \cdot (Ea^2 - Kb^2)^2}$$

B.9.a

$$C_2 = \left[\left(\frac{a^2 + b^2}{b^2}\right) \cdot E + K \right]^2$$

B.9.b

$$C_3 = -6 \cdot E \cdot \left[\left(\frac{a^2 + b^2}{b^2}\right) \cdot E + K \right]$$

B.9.c

$$C_4 = 9 \cdot E^2$$

B.9.d

57

Rewriting equation B.5 in terms of the constants C_1 through C_4 and substituting equation A.14 for ds, the equation for incremental strain energy due to a change in the cross-section becomes

$$dU_{xs} = \frac{2 \cdot E^1 \cdot I}{1 - \nu^2} \cdot C_1 \cdot db^2 \cdot \int_0^{\frac{\pi}{2}} \left[\frac{C_2}{(1 - k^2 \cdot \sin^2 \phi)^3} + \frac{C_3}{(1 - k^2 \cdot \sin^2 \phi)^4} + \frac{C_4}{(1 - k^2 \cdot \sin^2 \phi)} \right] \cdot a \cdot \sqrt{1 - k^2 \cdot \sin^2 \phi} \; d\phi$$

$$B.10$$

With further simplification, incremental strain energy due to sectional deformation is written as

$$dU_{xs} = \frac{2 \cdot E^1 \cdot I \cdot a}{1 - \nu^2} \cdot C_1 \cdot db^2 \cdot \int_0^{\frac{\pi}{2}} \left[\frac{C_2}{(1 - k^2 \cdot \sin^2 \phi)^{2.5}} + \frac{C_3}{(1 - k^2 \cdot \sin^2 \phi)^{3.5}} + \frac{C_4}{(1 - k^2 \cdot \sin^2 \phi)^{4.5}} \right] d\phi$$

$$B.11$$

All of the terms in the denominator of the integral in equation B.11 may be written in terms of elliptic functions by letting

$$\sin (\phi) = sn (u) \qquad\qquad B.12$$

and

58

$$\cos \cdot (\phi) = cn \cdot (u) \qquad\qquad\qquad\qquad \text{B.13}$$

so that

$$d(\sin\phi) = \cos\phi \cdot d\phi = d(sn(u)) = cn(u) \cdot dn(u) \cdot du \qquad\qquad \text{B.14}$$

Solving for $d\phi$,

$$d\phi = dn(u) \cdot du \qquad\qquad\qquad\qquad \text{B.15}$$

In addition,

$$1 - k^2 \cdot \sin^2 \cdot (\phi) = 1 - k^2 \cdot sn^2 \cdot (u) \qquad\qquad \text{B.16}$$

where

$$1 - k^2 \cdot sn^2 \cdot (u) = dn^2 \cdot (u) \qquad\qquad\qquad \text{B.17}$$

by definition in equation 2.4.b. Equation B.11 is further simplified by evaluating the integral in parts and by making substitutions with equations B.15 and B.17. The first term in the integral is written as

$$\int_0^{\frac{\pi}{2}} (1 - k^2 \cdot \sin^2 \phi)^{-2.5} \, d\phi = \int_0^K (dn^2(u))^{-2.5} \cdot dn(u) \, du$$

59

$$= \int_0^K (dn^{-5}(u) \cdot dn \cdot (u)) \ du = \int_0^K dn^{-4}(u) \ du \qquad \text{B.18}$$

Applying equation 5.131.3 from Ref. 14 for m = -4,

$$\int_0^K dn^{-4}(u) \ du =$$

$$-\frac{1}{3 \cdot (k^1)^2} \left[k^2 \cdot dn^{-3}(u) \cdot sn(u) \cdot cn(u) - 2 \cdot (2 - k^2) \cdot \int_0^K dn^{-2}(u) \ du + \int_0^K u \ du \right]$$

$$\text{B.19}$$

Using the elliptic function identities defined in Chapter I and the relationships

$$(k^1)^2 = 1 - k^2 \qquad \text{B.20}$$

and

$$\int_0^K (dn^2(u)) \ du = E \qquad \text{B.21}$$

as defined in Refs 9 and 10, equation B.18 is rewritten in simpler form as

$$\int_0^K dn^{-4}(u) \ du = -\frac{K}{3 \cdot (1 - k^2)} + \frac{2 \cdot (2 - k^2)}{3 \cdot (1 - k^2)} \cdot \int_0^K dn^{-2}(u) \ du \qquad \text{B.22}$$

Again, applying equation 5.131.3 from Ref. 14 to solve for the final integral where

60

$m = -2$, equation B.22 is further simplified to the expression

$$\int_0^K dn^{-4} \cdot (u)\, du = \frac{1}{3 \cdot (1 - k^2)} \cdot \left[\frac{2 \cdot E \cdot (2 - k^2)}{(1 - k^2)} - K \right]$$

B.23

where, for future reference,

$$\int_0^K dn^{-2} \cdot (u)\, du = \frac{E}{(1 - k^2)}$$

B.24

Still in the process of simplifying the equation for the incremental strain energy in Bourdons due to changes in cross-section, the next integral to be evaluated is

$$\int_0^{\frac{\pi}{2}} (1 - k^2 \cdot \sin^2 \cdot \phi)^{-3.5}\, d\phi = \int_0^K (dn^2 \cdot (u))^{-3.5} \cdot dn \cdot (u)\, du$$

$$= \int_0^K (dn^{-7} \cdot (u) \cdot dn \cdot (u))\, du = \int_0^K dn^{-6} \cdot (u)\, du$$

B.25

Applying equation 5.131.3 from Ref. 14 for $m = -6$,

61

$$\int_0^K dn^{-6}(u)\, du =$$

$$-\frac{1}{5\cdot(k^1)^2}\left[k^2\cdot dn^{-5}(u)\cdot sn(u)\cdot cn(u) - 4\cdot(2-k^2)\cdot\int_0^K dn^{-4}(u)\, du + 3\cdot\int_0^K dn^{-2}(u)\, du\right]$$

B.26

Substituting equations B.20, B.23, and B.24 and applying the elliptic function identities defined in Chapter I,

$$\int_0^K dn^{-6}(u)\, du = \frac{4\cdot(2-k^2)}{15\cdot(1-k^2)^2}\cdot\left[\frac{2\cdot E\cdot(2-k^2)}{(1-k^2)} - K\right] - \frac{3\cdot E}{5\cdot(1-k^2)^2}$$

B.27

And finally, applying the same procedure to the denominator of equation B.11 corresponding to the constant C_4,

$$\int_0^{\frac{\pi}{2}} (1 - k^2\cdot sin^2\phi)^{-4.5}\, d\phi = \int_0^K (dn^2(u))^{-4.5}\cdot dn(u)\, du$$

$$= \int_0^K (dn^{-9}(u)\cdot dn(u))\, du = \int_0^K dn^{-8}(u)\, du$$

B.28

where, applying equation 5.131.3 from Ref. 14 for m = -8,

$$\int_0^K dn^{-8} \cdot (u) \ du =$$

$$-\frac{1}{7 \cdot (k^1)^2} \cdot \left[k^2 \cdot dn^{-7} \cdot (u) \cdot sn(u) \cdot cn(u) - 6 \cdot (2 - k^2) \cdot \int_0^K dn^{-6} \cdot (u) \ du + 5 \cdot \int_0^K dn^{-4} \cdot (u) \ du \right]$$

<div align="right">B.29</div>

Substituting equations B.20, B.23, and B.27 and applying the elliptic function identities defined in Chapter I,

$$\int_0^K dn^{-8} \cdot (u) \ du = \left[\frac{24 \cdot (2 - k^2)^2}{105 \cdot (1 - k^2)^3} - \frac{5}{21 \cdot (1 - k^2)^2} \right] \left[\frac{2 \cdot E \cdot (2 - k^2)}{(1 - k^2)} - K \right] - \frac{18 \cdot E \cdot (2 - k^2)}{35 \cdot (1 - k^2)^3}$$

<div align="right">B.30</div>

The equation for incremental strain energy due to changes in cross-section may now be written as

$$dU_{xs} = \frac{2 \cdot a \cdot E^1 \cdot I \cdot C_1 \cdot db^2}{(1 - v^2)} \cdot \int_0^K \left[C_2 \cdot dn^{-4} \cdot (u) + C_3 \cdot dn^{-6} \cdot (u) + C_4 \cdot dn^{-8} \cdot (u) \right] du \qquad \text{B.31}$$

where the integrals of dn^{-4} (u), dn^{-6}(u), and dn^{-8} (u) are defined by equations 2.5, 2,6, and 2.7, respectively.

APPENDIX C. INCREMENTAL STRAIN ENERGY
DUE TO BENDING

As defined in Appendix B, the total strain energy due to bending in a beam is defined as

$$U = \int_0^L \frac{M^2}{2 \cdot E^1 \cdot I} \, dx \qquad \text{C.1}$$

where M represents the net moment acting on the bourdon as a result of pressurization and E^1 is Young's modulus. The detailed derivation of the net moment acting on the elastic element represents a very large segment of this appendix.

Referencing Figure 5, the elemental area of the bourdon tube is defined by the expression

$$dA = (R + \rho \cos\phi) \cdot d\theta \cdot ds \qquad \text{C.2}$$

Recalling equation A.14, equation C.2 may also be written as

$$dA = a \cdot (R + \rho \cos\phi) \cdot \sqrt{1 - k^2 \cdot \sin^2\phi} \cdot d\theta \cdot d\phi \qquad \text{C.3}$$

The force acting on the elemental area is defined as

$$\overrightarrow{dF} = \overrightarrow{P} \cdot dA \qquad \text{C.4}$$

where

$$\overrightarrow{P} = P \cdot ((\cos\alpha \cdot \cos\theta) \cdot i + (\cos\alpha \cdot \sin\theta) \cdot j + \sin\alpha \cdot k) \qquad \text{C.5}$$

The angle α describes the direction of the normal component of pressure acting on the wall of the tube as shown in Figure 5. Substituting equations C.3 and C.5 into equation C.4, the elemental force acting on the elemental area of the bourdon is

$$\overrightarrow{dF} = P \cdot ((\cos\alpha \cdot \cos\theta) \cdot i + (\cos\alpha \cdot \sin\theta) \cdot j + \sin\alpha \cdot k) \cdot \left[a \cdot (R + \rho \cdot \cos\phi) \cdot \sqrt{1 - k^2 \cdot \sin^2\phi} \cdot d\theta \cdot d\phi \right]$$

C.6

where the corresponding moment arm to the elemental area is defined as

$$\overrightarrow{dr} = -R \cdot (\cos\beta \cdot i + \sin\beta \cdot j) + (R + \rho \cdot \cos\phi) \cdot (\cos\theta \cdot i + \sin\theta \cdot j) + \rho \cdot \sin\phi \cdot k \qquad \text{C.7}$$

Relating the angle α to the angle ϕ in Figure 6,

$$\cos\alpha = \frac{\cos\phi}{\sqrt{1 - k^2 \cdot \sin^2\phi}}$$

C.8

and

$$\sin\alpha = \frac{b \cdot \sin\phi}{a \cdot \sqrt{1 - k^2 \cdot \sin^2\phi}}$$

C.9

As a result, equation C.6 may be expressed as

$$\overrightarrow{dF} = P \cdot a \cdot (R + \rho\cos\phi) \cdot \left[(\cos\phi \cdot \cos\theta) \cdot i + (\cos\phi \cdot \sin\theta) \cdot j + \frac{b}{a} \cdot \sin\phi \cdot k \right] \cdot d\phi \cdot d\theta$$

C.10

66

The moment acting on the elemental area due to an elemental force is defined by the equation

$$\overrightarrow{dM} = \overrightarrow{dr} \times \overrightarrow{dF}$$ C.11

Temporarily factoring out $Pa(R+\rho\cos\phi)d\phi d\theta$ from equation C.10 for simplicity, the vectorial components of the resulting cross product of equation C.11 are:

$$\left[\cos\phi \cdot \sin\theta \cdot \rho \cdot \sin\phi - \frac{b}{a} \cdot \sin\phi \cdot (R \cdot \sin\theta - R \cdot \sin\beta + \rho \cdot \cos\phi \cdot \sin\theta) \right] \cdot i$$ C.11.a

$$-\left[\cos\phi \cdot \cos\theta \cdot \rho \cdot \sin\phi - \frac{b}{a} \cdot \sin\phi \cdot (R \cdot \cos\theta - R \cdot \cos\beta + \rho \cdot \cos\phi \cdot \cos\theta) \right] \cdot j$$ C.11.b

and

$$((R \cdot \cos\theta - R \cdot \cos\beta + \rho \cdot \cos\phi \cdot \cos\theta) \cdot \cos\phi \sin\theta - \cos\phi \cos\theta \cdot (R \cdot \sin\theta - R \cdot \sin\beta + \rho \cdot \cos\phi \cdot \sin\theta)) \cdot k$$

C.11.c

For the sake of brevity, the cosine function will be abbreviated by "c" and the sine function will be abbreviated by "s" from this point to the end of Appendix C. Continued simplification begets the following equation for the moment acting on the bourdon tube:

$$M = \int_0^{2\cdot\pi} \int_0^{\beta} \left[P \cdot a \cdot (R + \rho \cdot c\phi) \cdot \left[\rho \cdot c\phi \cdot s\phi \cdot s\theta - \frac{b}{a} \cdot (R + \rho \cdot c\phi) \cdot s\phi \cdot s\theta + \frac{b}{a} \cdot R \cdot s\phi \cdot s\beta \right] \right] \cdot i \, d\theta \, d\phi$$

$$-\int_{0}^{2\cdot\pi}\int_{0}^{\beta}\left[P\cdot a\cdot(R+\rho\cdot c\phi)\cdot\left[\rho\cdot c\phi\cdot s\phi\cdot c\theta-\frac{b}{a}(R+\rho\cdot c\phi)\cdot s\phi\cdot c\theta+\frac{b}{a}R\cdot s\phi\cdot c\beta\right]\right]\cdot j\ d\theta\ d\phi$$

$$+\int_{0}^{2\cdot\pi}\int_{0}^{\beta}P\cdot a\cdot(R+\rho\cdot c\phi)\cdot R\cdot c\phi\cdot(c\theta\cdot s\beta-s\theta\cdot c\beta)\cdot k\ d\theta\ d\phi$$

C.12

Factoring back in the expression $Pa(R+\rho cos\phi)d\phi d\theta$ and evaluating the x-component of the equation C.12 first,

$$P\cdot a\cdot\int_{0}^{2\cdot\pi}\int_{0}^{\beta}(R+\rho\cdot c\phi)\cdot\left[\rho\cdot c\phi\cdot s\theta-\frac{b}{a}\cdot(R+\rho\cdot c\phi)\cdot s\theta+\frac{b}{a}\cdot R\cdot s\beta\right]\cdot s\phi\ d\theta\ d\phi=0$$

C.13

because $sin\phi$ is an odd function on the interval 0 to 2π. Similarly for the y-component of equation C.11,

$$-P\cdot a\cdot\int_{0}^{2\cdot\pi}\int_{0}^{\beta}(R+\rho\cdot c\phi)\cdot\left[\rho\cdot c\phi\cdot c\theta-\frac{b}{a}\cdot(R+\rho\cdot c\phi)\cdot c\theta+\frac{b}{a}\cdot R\cdot c\beta\right]\cdot s\phi\ d\theta\ d\phi=0$$

C.14

Evaluating the z-component of equation C.11,

68

$$P \cdot a \cdot R \cdot \int_{0}^{2 \cdot \pi} \int_{0}^{\beta} (R + \rho \cdot c\phi) \cdot c\phi \cdot (c\theta \cdot s\beta - s\theta \cdot c\beta) \, d\theta \, d\phi =$$

$$\frac{4 \cdot P \cdot a^2 \cdot R}{3} \cdot (1 - c\beta) \cdot \left[\frac{K - E}{k^2} + (2 \cdot E - K) \right]$$

C.15

Therefore, the final expression for the moment acting on the walls of the tube is

$$\overrightarrow{M} = \frac{4 \cdot P \cdot a^2 \cdot R}{3} \cdot (1 - c\beta) \cdot \left[\frac{K - E}{k^2} + (2 \cdot E - K) \right] \cdot k$$

C.16

Again referring to Figure 5, the net force acting on the end cap of the bourdon element is

$$\overrightarrow{F}_{cap} = -P \cdot \pi \cdot a \cdot b \cdot j$$

C.17

and the corresponding moment arm is

$$\overrightarrow{dr} = R \cdot (1 - c\beta) \cdot i - R \cdot s\beta \cdot j$$

C.18

Performing the cross product,

$$\overrightarrow{M}_{cap} = \overrightarrow{dr} \times \overrightarrow{dF}_{cap} = -P \cdot R \cdot \pi \cdot a \cdot b \cdot (1 - c\beta) \cdot k$$

C.19

69

Therefore, the net moment acting on the tube is the sum of the moments acting on the walls and end cap of the Bourdon as shown in next equation:

$$\overrightarrow{M_{net}} = \overrightarrow{M} + \overrightarrow{M_{cap}} = P \cdot a \cdot R \cdot (1 - c\beta) \cdot \left[\frac{4 \cdot a}{3} \cdot \left[\frac{K - E}{k^2} + (2 \cdot E - K) \right] - \pi \cdot b \right] \cdot k$$

C.20

For simplicity, the new variable D is defined as

$$D = a \cdot \left[\frac{4 \cdot a}{3} \cdot \left[\frac{K - E}{k^2} + (2 \cdot E - K) \right] - \frac{\pi \cdot b}{a} \right]$$

C.21

such that

$$\overrightarrow{M_{net}} = P \cdot a \cdot R \cdot D \cdot (1 - c\beta) \cdot k$$

C.22

Substituting equation C.22 into equation C.1, the total bending strain energy is expressed as

$$U_b = \int_0^\mu \frac{(P \cdot a \cdot R \cdot D \cdot (1 - c\beta))^2}{2 \cdot E^1 \cdot I} \cdot R \, d\beta$$

C.23

The incremental strain energy is calculated by differentiating U_b with respect to the dimensions a and b, the applied pressure P, and the radius of curvature of the tube R such that

70

$$dU_b = \left(\frac{d}{da}U\right) \cdot da + \left(\frac{d}{db}U\right) \cdot db + \left(\frac{d}{dP}U\right) \cdot dP + \left(\frac{d}{dR}U\right) \cdot dR \qquad \text{C.24}$$

where

$$\left(\frac{d}{da}U\right) \cdot da = \frac{P^2 \cdot a \cdot R^3 \cdot D}{4 \cdot E^1 \cdot I} \cdot (6 \cdot \mu - 8 \cdot \sin(\mu) + \sin(2 \cdot \mu)) \cdot \left(a \cdot \frac{d}{da}D + D\right) \cdot da \qquad \text{C.25}$$

$$\left(\frac{d}{db}U\right) \cdot db = \frac{P^2 \cdot a^2 \cdot R^3 \cdot D}{4 \cdot E^1 \cdot I} \cdot (6 \cdot \mu - 8 \cdot \sin(\mu) + \sin(2 \cdot \mu)) \cdot \left(\frac{d}{db}D\right) \cdot db \qquad \text{C.26}$$

$$\left(\frac{d}{dP}U\right) \cdot dP = \frac{P \cdot a^2 \cdot R^3 \cdot D^2}{4 \cdot E^1 \cdot I} \cdot (6 \cdot \mu - 8 \cdot \sin(\mu) + \sin(2 \cdot \mu)) \cdot dP \qquad \text{C.27}$$

and

$$\left(\frac{d}{dR}U\right) \cdot dR = \frac{3 \cdot P^2 \cdot a^2 \cdot R^2 \cdot D^2}{8 \cdot E^1 \cdot I} \cdot (6 \cdot \mu - 8 \cdot \sin(\mu) + \sin(2 \cdot \mu)) \cdot dR \qquad \text{C.28}$$

Summing equations C.25 - C.28 and simplifying, the incremental strain energy in the bourdon due to bending may be expressed as

$$dU_b = \frac{P \cdot a^2 \cdot R^2 \cdot D}{4 \cdot E^1 \cdot I} \cdot (6 \cdot \mu - 8 \cdot \sin(\mu) + \sin(2 \cdot \mu)) \times$$

$$\left[\frac{P \cdot R \cdot b \cdot (E - K)}{E \cdot a^2 - K \cdot b^2} \cdot \left(a \cdot \frac{d}{da} D + D \right) \cdot db + P \cdot R \cdot \left(\frac{d}{db} D \right) + R \cdot D \cdot dP + 1.5 (P \cdot D \cdot dR) \right]$$

C.29

where

$$\frac{d}{da} D = \frac{4}{3} \cdot \left[\frac{a^2 \cdot (K - E) \cdot (3 \cdot (a^2 - b^2) - 2 \cdot a^2)}{(a^2 - b^2)^2} - (2 \cdot E - K) \right]$$

C.30

and

$$\frac{d}{db} D = \frac{4}{3} \cdot \left[\frac{2 \cdot a^3 \cdot b \cdot (K - E)}{(a^2 - b^2)^2} - \pi \right]$$

C.31

as a result of taking the partial derivatives of equation C.21 with respect to the semi-major and minor axes, respectively.

APPENDIX D. DEVELOPING EQUATIONS FOR TIP TRAVEL

Two equations are used to develop the equation for Bourdon tip displacement.
The first equation is based on the assumption made in this analytical study that the length
of the elastic element remains constant during pressurization. Based on this assumption,
the following is true:

$$\mu \cdot R = Constant \hspace{4cm} D.1$$

and

$$\mu \cdot dR + R \cdot d\mu = 0 \hspace{4cm} D.2$$

where incremental tip travel, dR, is expressed as

$$dR = \frac{-R \cdot d\mu}{\mu} \hspace{4cm} D.3$$

Referring to Figure 6, the variables R and μ are measurable quantities but $d\mu$ must
be calculated. One way to do so is to apply Castigliano's Second Theorem as defined in
Ref. 11 which states that

$$\theta_i = \int_0^L \frac{M}{E^1 \cdot I} \left(\frac{d}{dM_i} M \right) dx \hspace{3cm} D.4$$

where M_i is an imaginary moment and E^1 is Young's modulus. This equation is helpful
because, in beam theory, θ_i represents the change in the slope of the elastic member at
the point of an applied imaginary moment. Geometry then dictates that

$$d\mu = -\theta_i \quad\quad\quad\quad\quad\quad\quad\quad\quad\quad\quad\quad\quad D.5$$

thereby establishing the second equation necessary to calculate tip deflection. Modeling the Bourdon as a beam, this relationship makes sense because as the radius of curvature at the tip of the Bourdon becomes larger with pressure, the change in slope becomes larger and the angle μ describing the length of the elastic element becomes smaller. Therefore, once ϕ_i is known, bourdon tip displacement is calculated using equation D.3.

Continuing with the application of Castigliano's second theorem, a dummy moment M_i is applied in the direction chosen positive for θ_i so that the bending moment in equation D.4 becomes

$$\vec{M} = -P \cdot a \cdot R \cdot D \cdot (1 - \cos\beta) \cdot k - M_i \cdot k \quad\quad\quad\quad\quad D.6$$

and

$$\frac{d}{dM_i} M = -1 \quad\quad\quad\quad\quad\quad\quad\quad\quad\quad\quad D.7$$

Making the appropriate substitutions into equation D.4, setting M_i equal to zero, and integrating,

$$\theta_i = \frac{P \cdot a \cdot R \cdot D}{E^1 \cdot I} \cdot \int_0^\mu (1 - \cos\beta) \, d\beta = \frac{P \cdot a \cdot R \cdot D}{E^1 \cdot I} \cdot (\mu - \sin\mu)$$

$$D.8$$

74

A positive value of θ_i means the tip angle of rotation has the same sense of direction as the applied dummy moment. Because θ_i is a function of the dimensions a and b (a function of b because D is a function of b), an iterative solution for tip travel incorporates the cross-sectional deformation that occurs simultaneously with straightening.

APPENDIX E. FORTRAN SOURCE CODE

Program Bourdon

* This program calculates tip deflection in low pressure, C-type Bourdon
* elements for user-defined properties, geometries, and pressures.
*
*
*
* Definition of variables:
*
*   a = semi-major axis of the elliptical thin-walled tube (ID)
*   b = semi-minor axis of the elliptical thin-walled tube (ID)
*   t = wall thickness of elliptical tube
*   R = tip radius of curvature of the elliptical tube
*   p = internal pressure applied to the tube
*   mixs = I, the area moment of inertia of the tube for cross-sectional
*   deformation
*   mib = I, the area moment of inertia of the tube for bending
*   mu = arclength of the elliptical tube
*   epr = elastic modulus of the tube material
*   nu = poisson's ratio of the tube material
*   rad = input variable for the initial radius of curvature
*   rin = initial radius of curvature expressed in meters
*   da = incremental change in a
*   db = incremental change in b
*   dR = incremental change in R
*   dp = incremental internal pressure applied to the tube
*   dmu = incremental change in mu
*
*   smk = k, defined as the square root of 1-(b/a)^2
*   bk = K, Jacobian Elliptic Integral of the 1st kind
*   be = E, Jacobian Elliptic Integral of the 2nd kind
*
*   c1 = a constant in the expression for capc
*   c2dn = the product of a constant and the elliptic integral of
*   dn(u)e-4 in the expression for capc
*   c3dn = the product of a constant and the elliptic integral of
*   dn(u)e-6 in the expression for capc
*
*   c4dn = the product of a constant and the elliptic integral of
*   dn(u)e-8 in the expression for capc

77

```
*        D = a constant in the net moment equation expressed as a
*              function of a, b, K, and E
*        dDda = partial derivative of D wrt a
*        dDdb = partial derivative of D wrt b
*
*        capa = a constant expressed as a function of parameters a, b,
*            P, and R used in Subroutine Bndenrg
*        capb = a constant expressed as a function of parameters a, b,
*            P, and R used in Subroutine Bndenrg
*        capc = a constant expressed as a function of dimensions a and
*            b used in Subroutine Xsecenrg
*        capj = an expression representative of incremental external work
*        capl = the ratio of capj to capa used in the expression for capy
*        capx = the ratio of capc to capa used in the final expression
*            for db
*        capy = an expression representing the difference in capb and
*            capl used in the final expression for db
*        capz = a constant expressed as a function of parameters a, b,
*            P, and R used in Subroutine Bndenrg
*        thetai = bourdon tip rotation due to applied dummy moment
*
*        dV = volumetric change in the tube, dV = vol*db
*        duxs = change in internal energy due to a change in the
*            cross-section of the elliptical tube as a result
*            of an applied internal pressure
*        dub = change in internal energy due to bending of the
*             elliptical tube
*
*

      implicit real*8 (a-h,o-z)
       real*8 mixs, mib, mu, nu, maj, min

       common a,b,smk,bk,be,epr,R,mixs,mib,mu,nu,p,capc,capa,capb,capz,c1,
     +  c2dn,c3dn,c4dn,D,dDda,da,dDdb,pi,dp,dR,db,dmu,thetai,vol,capj,
     +  capl,capx,capy
*
       open (7,file='data',status='old')
       read (7,*)maj,min,wl,rad,mu,dp,pmax,epr,nu
       close (7)
*
* Dimensions converted to meters.
*
       a = maj/1000.0
       b = min/1000.0
```

```
          t = wl/1000.0
          rin = rad/1000.0
          R = rin
*
          call capke
*
          pi = 3.141592654
*
          vol = pi*a*(((a**2 + b**2)*be - 2.0*bk*b**2)/(be*a**2
     +        - bk*b**2))
*
          smk = sqrt(1.0 - (b/a)**2)
          mi = (pi/4.0)*((a + t)*(b + t)**3 - a*b**3)
*
*   This loop increases the internal pressure to a pre-determined
*   maximum pressure in increments of dp so that associated changes
*   in the variables a, b, R, and mu may be considered in the problem.
*
          Open(4,file='data',status='new')
*
          Do 10 p=0.0,pmax - dp,dp
             call capke
*
             vol = pi*a*(((a**2 + b**2)*be - 2.0*bk*b**2)/(be*a**2
     +           - bk*b**2))
*
             call xsecenrg
             call dercapd
             call dummy
             call tip
             call bndenrg
*
             capj = (p + dp)*vol
             capl = capj/capa
             capx = capc/capa
             capy = capb - capl
*
*   The final expression for db is written as a quadratic equation for
*   both roots of the equation.
*
             db = (-capy + sqrt(capy**2 - 4.0*capx*capz))/(2.0*capx)
*            db = (-capy - sqrt(capb**2 - 4.0*capx*capz))/(2.0*capx)
             da = (a*b*(be - bk)/(be*a**2 - bk*b**2))*db
```

79

```fortran
*   Variables incremented through the loop.
*
          a = a + da
          b = b + db
          R = R + dR
          mu = mu + dmu
          smk = sqrt(1.0 - (b/a)**2)
          mixs = t**3/12.0
          mi b= (pi/4.0)*((a + t)*(b + t)**3 - a*b**3)
*
10        continue
*
          close (4)
*
          stop
          end
*


          Subroutine Capke
*
*   This subroutine calculates K and E, elliptic integrals of the first
*   and second kind, respectively.  K and E are functions of k which is
*   itself a function of the major (2a) and minor (2b) axes of the
*   ellipse.
*
          implicit real*8 (a-h,o-z)
          real*8 mixs, mib, mu, nu

          common a,b,smk,bk,be,epr,R,mixs,mib,mu,nu,p,capc,capa,capb,capz,c1,
      +   c2dn,c3dn,c4dn,D,dDda,da,dDdb,pi,dp,dR,db,dmu,thetai,vol,capj,
      +   capl,capx,capy

*
          ang = asin(smk)
          eps = 1.0e-8
          a0 = 1.0
          b0 = cos(ang)
          c0 = sin(ang)
          rmult = 1.0
          stor = c0**2
          bk = 1.5707963
          be = bk*(1.0 - 0.5*stor)
89        if (abs(c0).lt.eps) goto 99
          a1 = 0.5*(a0 + b0)
```

```
        b1 = sqrt(a0*b0)
        c1 = 0.5*(a0 - b0)
        rmult = 2.0*rmult
        stor = stor + rmult*(c1**2)
        bk = 1.5707963/a1
        be = bk*(1.0 - 0.5*stor)
        a0 = a1
        b0 = b1
        c0 = c1
        goto 89
*
  99    continue
        return
        end
*


        Subroutine Xsecenrg
*
*  This subroutine calculates the change in internal energy due to a
*  change in the cross-sectional area of an elliptic tube when an
*  internal pressure (greater than external or ambient pressure) is
*  applied to the tube.  The change in internal energy occurs when
*  the elliptical cross-section becomes more cicular with applied pres-
*  sure.
*
        implicit real*8 (a-h,o-z)
        real*8 mixs, mib, mu, nu

        common a,b,smk,bk,be,epr,R,mixs,mib,mu,nu,p,capc,capa,capb,capz,c1,
     +  c2dn,c3dn,c4dn,D,dDda,da,dDdb,pi,dp,dR,db,dmu,thetai,vol,capj,
     +  capl,capx,capy
*
        call jacconst
*
        capc = (2.0*a*epr*mixs*c1*(c2dn + c3dn + c4dn))/(1.0 - nu**2)
*
*  The change in internal energy due to a change in the cross-section
*  is defined as duxs = capc*db**2
*
        return
        end
```

81

```
        Subroutine Jacconst
*
*   This subroutine simplifies the expression needed to calculate the
*   change in internal energy due to a change in the tube's cross-
*   section. C1 is a constant for specific major and minor axes of
*   the elliptical tube.  Constants c2nd, c3dn, and c4dn are
*   also specific for given tube axes but also include the evaluation
*   of the elliptic trigonometric function dn(u) raised to the -4, -6,
*   and -8 powers, respectively.
*
        implicit real*8 (a-h,o-z)
        real*8 mixs, mib, mu, nu

        common a,b,smk,bk,be,epr,R,mixs,mib,mu,nu,p,capc,capa,capb,capz,c1,
     +  c2dn,c3dn,c4dn,D,dDda,da,dDdb,pi,dp,dR,db,dmu,thetai,vol,capj,
     +  capl,capx,capy
*
        c1 = (b/a)**4*(1.0/(be*a**2 - bk*b**2)**2)
        c2 = (((a**2 + b**2)/b**2)*be + bk)**2
        c3 = -6.0*be*(((a**2 + b**2)/b**2)*be + bk)
        c4 = 9.0*be**2
*
        dn2 = (2.0*be*(2.0 - smk**2)/(1.0 - smk**2) - bk)/(3.0*(1.0 -
     +      smk**2))
        dn3 = (4.0*(2.0 - smk**2)/(15.0*(1.0 - smk**2)**2))*(2.0*be*(2.0
     +      - smk**2)/(1.0 - smk**2) - bk) - (3.0*be/(5.0*(1.0 - smk
     +      **2)**2))
        dn4 = (24.0*(2.0 - smk**2)**2/(105.0*(1.0 - smk**2)**3) - 5.0/
     +      (21.0*(1.0 - smk**2)**2))*(2.0*be*(2.0 - smk**2)/(1.0 -
     +      smk**2) - bk) - (18.0*be*(2.0 - smk**2)/(35.0*(1.0 - smk**2)**3))
        c2dn = c2*dn2
        c3dn = c3*dn3
        c4dn = c4*dn4
*
        return
        end
*


        Subroutine Dummy
*
*   This subroutine calculates the change in the slope at the free end
*   of the tube using Castigliano's second theorem.  The change in the
*   slope is determined by applying a dummy moment at the tube tip and
*   incorporating that moment into the internal energy equation for a
```

```
*   beam.  Thetai is found by integrating the internal energy equation and
*   then setting the dummy moment equal to zero.
*
        implicit real*8 (a-h,o-z)
        real *8 mixs, mib,nu, mu

        common a,b,smk,bk,be,epr,R,mixs,mib,mu,nu,p,capc,capa,capb,capz,c1,
     +  c2dn,c3dn,c4dn,D,dDda,da,dDdb,pi,dp,dR,db,dmu,thetai,vol,capj,
     +  capl,capx,capy
*
        thetai = ((p + dp)*a*(R**2)*D*(mu - sin(mu)))/(epr*mib)
*
*   Thetai should be a positive value to indicate that the angle of
*   rotation has the same sense of direction as the applied dummy moment.
*
        return
        end
*


        Subroutine Tip
*
*   Once thetai is known, the tip deflection of the tube can be
*   calculated by assuming that mu*R = constant.  In doing so,
*   mu*dR + R*dmu = 0 must be true.  Geometry shows that mu has the
*   same magnitude but opposite sense of thetai.
*
        implicit real*8 (a-h,o-z)
        real *8 mixs, mib, nu, mu

        common a,b,smk,bk,be,epr,R,mixs,mib,mu,nu,p,capc,capa,capb,capz,c1,
     +  c2dn,c3dn,c4dn,D,dDda,da,dDdb,pi,dp,dR,db,dmu,thetai,vol,capj,
     +  capl,capx,capy
*
        dmu = -thetai
*
        dR = (-R*dmu)/mu
*
        return
        end
```

```fortran
      Subroutine Bndenrg
*
*  This subroutine simplies the expression needed to calculate the
*  change in internal energy due to bending in the tube.  Capa, capb,
*  and capz are all constant for the given parameters but change as the
*  parameters change.
*
      implicit real*8 (a-h,o-z)
      real *8 mixs, mib, nu, mu

      common a,b,smk,bk,be,epr,R,mixs, mib,mu,nu,p,capc,capa,capb,capz,c1,
     + c2dn,c3dn,c4dn,D,dDda,da,dDdb,pi,dp,dR,db,dmu,thetai,vol,capj,
     + capl,capx,capy
*
      capa = (((p + p)*(a**2)*(R**2)*D)*(6.0*musin(mu)+sin(2.0*mu)))/
     +        (4.0*epr*mi)

*
      capb = (((p + dp)*R*b*(be - bk)/(be*a**2 - bk*b**2))*(a*dDda +
     +     D)) + ((p + dp)*R*dDdb)
*
      capz = (R*D*dp) + (1.5*(p + dp)*D*dR)
*
*  The change in internal energy due to bending is defined as
*  dub = capa*(capb*db + capz)
*
      return
      end
*


      Subroutine Dercapd
*
*  This subroutine simplifies the expression for the net moment acting
*  on the tube as a result of the applied internal pressure.  D is the
*  simplifying term in the moment equation.  dDda and dDdb are the
*  partial derivatives of D with respect to a and b, respectively.
*
      implicit real*8 (a-h,o-z)
      real*8 mixs, mib, mu, nu

      common a,b,smk,bk,be,epr,R,mixs,mib,mu,nu,p,capc,capa,capb,capz,c1,
     + c2dn,c3dn,c4dn,D,dDda,da,dDdb,pi,dp,dR,db,dmu,thetai,vol,capj,
     + capl,capx,capy
```

84

```
      D = a*((4.0/3.0)*((bk - be)/(smk**2) + (2.0*be - bk)) - pi*(b/
   +    a))
      dDda = (4.0/3.0)*(((a**2*(bk - be)*(3.0*(a**2 - b**2) - 2.0*a**
   +    2))/(a**2 - b**2)**2) - (2.0*be - bk))
*
      dDdb = (4.0/3.0)*((2.0*a**3*b*(bk - be)/(a**2 - b**2)**2) - pi)
*
      return
      end
```

LIST OF REFERENCES

1. Hartland, P.W., *Pressure Gauge Handbook*, Marcel Dekker, Inc., 1985.

2. Heise, Dresser Industries Instrument Division, Newtown, CT.

3. ASME B.40.1, *Gauges - Pressure Indicating Dial Type - Elastic Element*, 1991.

4. Jimenez-dominguez, H., Figueroa-Lara, F., and Galindo, S., "Bourdon Gauge Absolute Manometer", *Instituto Nacional de Investigaciones Nucleares*, pp. 499, Nov., 1985.

5. Stewart Warner Instrument Corporation, Mt. Prospect, IL.

6. Wika Instrument Corporation, Lawrenceville, GA.

7. Giacobbe, J. B. and Bounds, A. M., "Material Selection Factor Significant in Bourdon Tubes", *Journal of Metals*, pp. 1147, Nov., 1952.

8. Wolf, Alfred, "An Elementary Theory of the Bourdon Gage", *Journal of Applied Mechanics*, pp. A-207, Sep., 1946.

9. Bowman, F., *Introduction to Elliptic Functions with Applications*, English Universities Press LTD, London, 1953.

10. Byrd, P.F. and Friedman, M.D., *Handbook of Elliptic Integrals for Engineers and Scientists, 2nd Ed.*, Springer-Verlag Berlin, 1971.

11. Logan, D.L., *Mechanics of Materials*, Harper Collins Publishers, 1991.

12. Andreeva, L.E., *Elastic Elements of Instruments*, Daniel Davey & Co., Inc., N.Y., 1966.

13. Ribreau, C., Naili, S., Bonis, M., and Langlet, A., "Collapse of Thin-Walled Elliptical Tubes for High Values of Major-to-Minor Axis Ratio", *Journal of Biomechanical Engineering*, pp. 432, Vol. 115, Nov., 1993.

14. Gradshtayn, I.S. and Ryzhik, I.M., *Table of Integrals, Series, and Products*, Academic Press, Inc., San Diego, CA, 1980.

INITIAL DISTRIBUTION LIST

No. Copies

1. Defense Technical Information Center   2
   8725 John J. Kingman Rd., STE 0944
   Ft. Belvoir, VA 22060-6218

2. Library, Code 13   2
   Naval Postgraduate School
   Monterey, CA 93943-5101

3. Department Chairman, Code ME   2
   Department of Mechanical Engineering
   Naval Postgraduate School
   Monterey, CA 93942-5000

4. Professor Ranjan Mukherjee   1
   Department of Mechanical Engineering
   Naval Postgraduate School
   Monterey, CA 93942-5000

5. Curricular Officer, Code 34   1
   Department of Mechanical Engineering
   Naval Postgraduate School
   Monterey, CA 93942-5000

6. LT Cynthia D. Conway   1
   33 McCauley Rd.
   Travelers Rest, SC 29690